Biochemistry and Biophysics Reports 42 (2025) 102007

Contents lists available at ScienceDirect

Biochemistry and Biophysics Reports

journal homepage: www.elsevier.com/locate/bbrep

Transcriptomic signatures of atheroresistance in the human atrium and ventricle highlight potential candidates for targeted atherosclerosis therapeutics

Paul A. Brown

Department of Basic Medical Sciences, Faculty of Medical Sciences Teaching and Research Complex, The University of the West Indies, Mona, Kingston 7, Jamaica

ARTICLE INFO

Keywords:
Transcriptome
Differential gene expression
Atherosclerosis
Immune cells
Endocardium
Endothelial dysfunction

ABSTRACT

Atherosclerosis risk is not uniform throughout the cardiovascular system. This study therefore aimed to compare the transcriptomes of atheroresistant human atrium and ventricle with atheroprone coronary arteries to identify transcriptomic signatures of atheroresistance and potential targets for atherosclerosis therapeutics. Using publicly available gene read counts, differentially expressed genes between the atrium, ventricle, and coronary artery were identified for each contrast and validated against the Swiss Institute of Bioinformatics' Bgee database. Over-representation analysis and active-subnetwork-oriented enrichment assessment then identified enriched terms, which were grouped into endothelial dysfunction-related processes. Potential biological significance was further explored with pathway analysis. Among 21474 features, 12656 differentially expressed genes were identified across the three contrasts and associated with 1215 enriched terms. There were 315 down-regulated and 133 up-regulated genes associated with endothelial dysfunction-related processes across the contrasts, including immune modulators, cell adhesion molecules, and lipid metabolism- and coagulation-related molecules. Differentially expressed genes were associated with six down-regulated Kyoto Encyclopedia of Genes and Genomes pathways, related to immune cell and associated endothelium functions. Review of regulated genes associated with endothelial dysfunction-related processes and included in these pathways, indicate immune cell-associated B cell scaffold protein with ankyrin repeats 1, as well as arterial endothelial cell-associated vascular cell adhesion molecule 1 and cadherin 5, as potential atherosclerosis targets.

1. Introduction

Atherosclerosis has long been understood as more than a vascular lipid storage disease, with increased awareness of other important pathogenic components including chronic inflammation and autoimmunity [1,2]. Important pro-atherogenic processes include increased endothelial permeability, endothelial cell (EC) LDL uptake and accumulation of oxidized LDL (oxLDL), monocyte recruitment and transendothelial migration, vascular inflammation, and coagulation [1,3]. Notwithstanding this improved understanding of the molecular mechanisms of this pathology, atherosclerosis remains the leading cause of cardiovascular and overall mortality [4].

This incongruence may be at least partly rooted in our often-systemic approach to atherosclerosis, even though within the cardiovascular system (CVS), the risk is not uniform. Atherosclerosis occurs rarely in the venous system and pulmonary artery, which are exposed only to venous blood [5]. There are also relatively atheroresistant (mostly upper limb) and atheroprone (neck, most thoraco-abdominal and lower limb) arteries [6]. Further, within the heart, there are the atheroresistant atria and ventricles, and the atheroprone coronary arteries, where atherosclerosis has been documented as early as the third decade of life [7]. These are important observations because, as with the venous system, the atria and ventricles appear vulnerable to factors with the potential to promote atherosclerosis. Like the coronary arteries, the heart chambers are often exposed to chronic hyperlipidemia [8], and less frequently to episodes of inflammation [9], and a pro-coagulant environment (atrial fibrillation) that promotes intracardiac thrombosis [10]. However, even within these contexts, the heart chambers are not prone to atherosclerosis. This implies that there is much to learn regarding the prevention of atherosclerosis, from an improved understanding of relevant aspects of the molecular biology of the heart.

A recent study of several major arteries demonstrated that transcriptomic differences between coronary and aortic arteries compared with the tibial artery, involved various genes related to immunity and

E-mail address: paul.brown02@uwimona.edu.jm.

https://doi.org/10.1016/j.bbrep.2025.102007
Received 26 December 2024; Received in revised form 28 March 2025; Accepted 4 April 2025

inflammation, with some contribution from genes related to membrane biology, lipid metabolism, and coagulation [11]. These variations could help explain documented dissimilarity in atherosclerosis risk across the CVS [5,6]. The current study expanded on this finding by exploring differences between the human atrium and ventricle, versus the coronary arteries. Several studies have examined the transcriptomic basis of atherosclerosis by looking for mechanisms of increased risk in atheroprone regions of the CVS [11–13]. This study took an alternate approach. It explored the transcriptomic basis of atheroresistance by looking for mechanisms of protection against atherosclerosis in the resistant heart chambers, which to the best of this author's knowledge has not previously been documented. Understanding why some CVS regions do not develop or are not prone to atherosclerosis, could not only support previously identified genes, but identify novel potential candidates, for targeted therapeutic strategies applicable to atheroprone regions of the CVS.

However, a major challenge of targeting atherosclerosis, is that the atherogenic process, which involves a robust LDL-induced monocyte-driven inflammatory response (LIMDIR) within arteries [1], is similar in many respects to the microbe-induced granulocyte-driven inflammatory response (MIGDIR) that occurs mostly in postcapillary venules [14]. Non-specific targeting of LIMDIR may therefore compromise MIGDIR, with dire consequences including immunosuppression [15–19]. This present study therefore aimed to compare the transcriptomes of the atheroresistant human atrium and ventricle with that of the atheroprone coronary arteries, to identify transcriptomic signatures of atheroresistance in the heart chambers, and associated molecular targets whose modulation has the potential to moderate development of arterial LIMDIR, without compromising postcapillary venular MIGDIR.

2. Methods

2.1. Study data

This study involved bioinformatic analysis of Genotype-Tissue Expression (GTEx) project data [20]. The datasets used (GTEx Analysis V8: dbGaP Accession phs000424.v8.p2) were downloaded on May 7th, 2024, and comprised gene read counts from grossly normal post-mortem samples [21] of human right atrial appendage [22], coronary arteries (left and right) [23], and anterior left ventricle [24], together with sample [25] and subject [26] data. Read counts (V8) were generated as previously reported [27,28], and described in detail at https://gtexportal.org/home/methods. The read count data consisted of 54592 genetic features (rows) and 1101 samples (columns), of which 429, 240, and 432 were atrium, coronary, and ventricle samples. There were 63 variables among the sample attributes, including SMTSD (Tissue Type: the grouping variable), batch-related variables (e.g. RNA isolation process and analysis date), quality-related variables [autolysis score and RNA Integrity Number (RIN)], as well as mapping- and sequence-related variables. The subject phenotypes were sex, age, and Hardy scale.

2.2. Bioinformatic analysis

The bioinformatic analysis closely followed the methodology of a previous report that compared gene counts between several major arteries [11]. Atrium, coronary, and ventricle data files downloaded from the GTEx Portal were merged and converted into a SummarizedExperiment object using the packages *cmapR* [version 1.14.0], [29], *org.Hs.eg.db* [version 3.18.0] [30] and *SummarizedExperiment*, [version 1.32.0] [31]. An intermediate GCT data object was created from the merged database with the cmapR package (*new* function), using human org.Hs.eg.db database annotation information. Finally, the GCT data object was converted into a SummarizedExperiment object (*as* function) for data cleaning. Based on initial exploratory analysis, this database was filtered using logical indexing, to remove samples with more than mild autolysis, retain only those samples with a recorded Hardy classification and an RIN (RNA quality) $\geq$6, and retain only features with gene counts $\geq$10 in $\geq$206 (sample count of smallest SMTSD group after previous filtering steps) samples. The RIN cutoff was guided by the GTEx documentation, that considered sample RIN $\geq$6 as adequate for RNA sequencing analysis [27]. The dimensions of the resulting dataset were 21779 rows (features) and 962 columns (samples), with 394, 206, and 362 atrium, coronary, and ventricle samples, respectively. With respect to batch-related variables, initial analysis also revealed use of 2 RNA isolation procedures and 175 RNA analysis dates as well as significant associations between these variables and tissue type (grouping variable). All five batch-related variables (RNA isolation ID, procedure, and date as well as analysis ID and date) were also significantly associated with RIN. Due to the potential impact of the quality-, batch-, and phenotype-related variables, as well as significant associations between the grouping variable and several of these variables, a DeSeqDataSet object was constructed from the cleaned SummarizedExperiment object, with the *DeSeq2* package [version 1.42.1] [32], while controlling for RIN, RNA isolation procedure and analysis date, as well as subject phenotypes (sex, age and Hardy scale). These potential confounders were entered into the design formula during DeSeqDataSet object construction (*DESeqDataSet* function), to ensure that the study findings were not influenced by these variables.

The *DESeq* function of the *DeSeq2* package [32] was used for differential gene expression (DGE), with data from the DeSeqDataSet object. Results were extracted (*results* function) for three contrasts, adjusting p-values with the Benjamini & Hochberg procedure [33]: atrium vs. coronary (AC), ventricle vs. coronary (VC), and atrium vs. ventricle (AV). A total of 305 non-converging genetic features, with significantly higher counts (Welch Two Sample *t*-test: 13849.21 vs. 2956.63, $t = 3.0394$, $p < 0.05$) and zero (0) counts for each feature (Welch Two Sample *t*-test: 14.7 % vs.1.7 %, $t = 16.625$, $p < 0.05$, were removed, having not been excluded during the initial filtering step to retain features with gene counts $\geq$10 in $\geq$206 samples. Dimensions of the final filtered dataset were 21474 rows and 962 columns, with 394, 206, and 362 atrium, coronary, and ventricle samples, respectively. Differentially expressed genes (DEGs) were specified by adjusted p value/false discovery rate (FDR) < 0.05 [33] and absolute $\log^2$ fold change $\geq$1.0. The *pheatmap* package [version 1.0.12] [34] visualized the DEG heatmaps.

DEGs identified for each contrast were then subjected to over-representation analysis (ORA) with the *enrichGO* function of the *clusterProfiler* package [version 4.10.1] [35,36] targeting the Gene Ontology (GO) knowledgebase [37,38] and active-subnetwork-oriented enrichment analysis (ASOEA) with the *active_snw_search* function of the *pathfindR* package [version 2.4.1] [39], adjusting p-values with the Benjamini & Hochberg procedure [33]. For ORA, enriched categories were identified using a background gene list of all 21474 features to test DEGs for each contrast. With respect to ASOEA, active subnetworks were identified for each contrast by mapping the associated DEGs unto the BioGRID protein–protein interaction network with the "greedy search" algorithm. GO categories and ASOEA terms below an FDR of 0.005 [33] were identified as enriched, and visualized with *ggplot* function [version 3.5.1] from the *ggplot2* package [40] and *enrichment_chart* function from the *pathfindR* package [39], respectively. Relevant enriched ORA (GO) and ASOEA terms were grouped into endothelial dysfunction (ED)-related processes (immunity/inflammation, membrane integrity, lipid metabolism, and coagulation) for each contrast. Genes associated with GO/ASOEA terms for each category (process) were filtered from the list of DEGs, and visualized with *pheatmap* package [34]. Finally, these genes were compared across category and contrast, to further evaluate transcriptional relationships between tissues.

The validity of categorizing enrichment terms was tested by contrasting DEGs identified for each category with related listings of gene symbols and aliases. Gene symbols were obtained from the Comparative Toxicogenomics Database on June 25th, 2024 [41]. Relevant datasets were obtained from the "Diseases" section, using the search terms,

"inflammation," "edema" (impaired membrane integrity proxy), "dyslipidemias," and "blood coagulation disorders." Gene synonyms were then added *humanSyno* and *alias2Symbol* functions; *geneSynonym* and *limma* packages [42,43]; version 1.7.24.6.23 and 3.58.1, respectively. Validation of top regulated genes for each category and contrast was against their documented relative expression reported by Swiss Institute of Bioinformatics' Bgee database [44]. Finally, possible biological relevance was assessed by comparing DEGs linked to GO/ASOEA terms, for all categories and contrasts.

Potential biological significance was further explored by pathway analysis [*gage* package (version 2.52.0)] [45,46] using the Kyoto Encyclopedia of Genes and Genomes (KEGG) Database (https://www.genome.jp/kegg/pathway.html), to find up- or down-regulated pathways associated with the three sets of contrast DEGs. The *gage* function utilized the $\log^2$ fold change data for the set of contrast DEGs, with the "same.dir" parameter set to "True", which tests for coregulation of genes within the gene set, i.e. genes up or down regulated [45]. Pathways below an FDR q-value of 0.05 [33] were considered significantly regulated and visualized [*pathview* package, version 1.42.0] [47]. The relative expression of DEGs associated with GO/ASOEA terms as well as with significantly regulated pathways were compared with previously documented expression in the Bgee database [44]. Finally, DEGs of interest were reviewed, with focus on DEGs linked to GO/ASOEA terms, that were also identified in regulated KEGG pathways.

2.3. Statistical analysis

The relationships between SMTSD (Tissue Type), and other variables were evaluated with ANOVA or Fisher exact test, and those between RIN and other variables with ANOVA, Pearson correlation, or the *t*-test. Negative binomial GLM fitting, with the Wald test [32], was used to identify differentially expressed genes. All data preprocessing, statistical analysis, and data visualization were conducted with R v4.3.2 (The R Foundation, 2023). A p value of <0.05 was considered significant. However, adjusted p values were used (Benjamini & Hochberg procedure [33]), controlling the FDR at thresholds of 0.05, 0.005 and 0.05, respectively, for identification of DEGs, enriched GO and ASOEA terms, and regulated pathways.

3. Results

3.1. Descriptive analysis

There were 21474 rows (features) and 962 columns (samples) in the final dataset. The study sample included 34.2 % females (Fig. 1a). The 20–29, 30–39, 40–49, 50–59, 60–69, and 70–79 age ranges contained

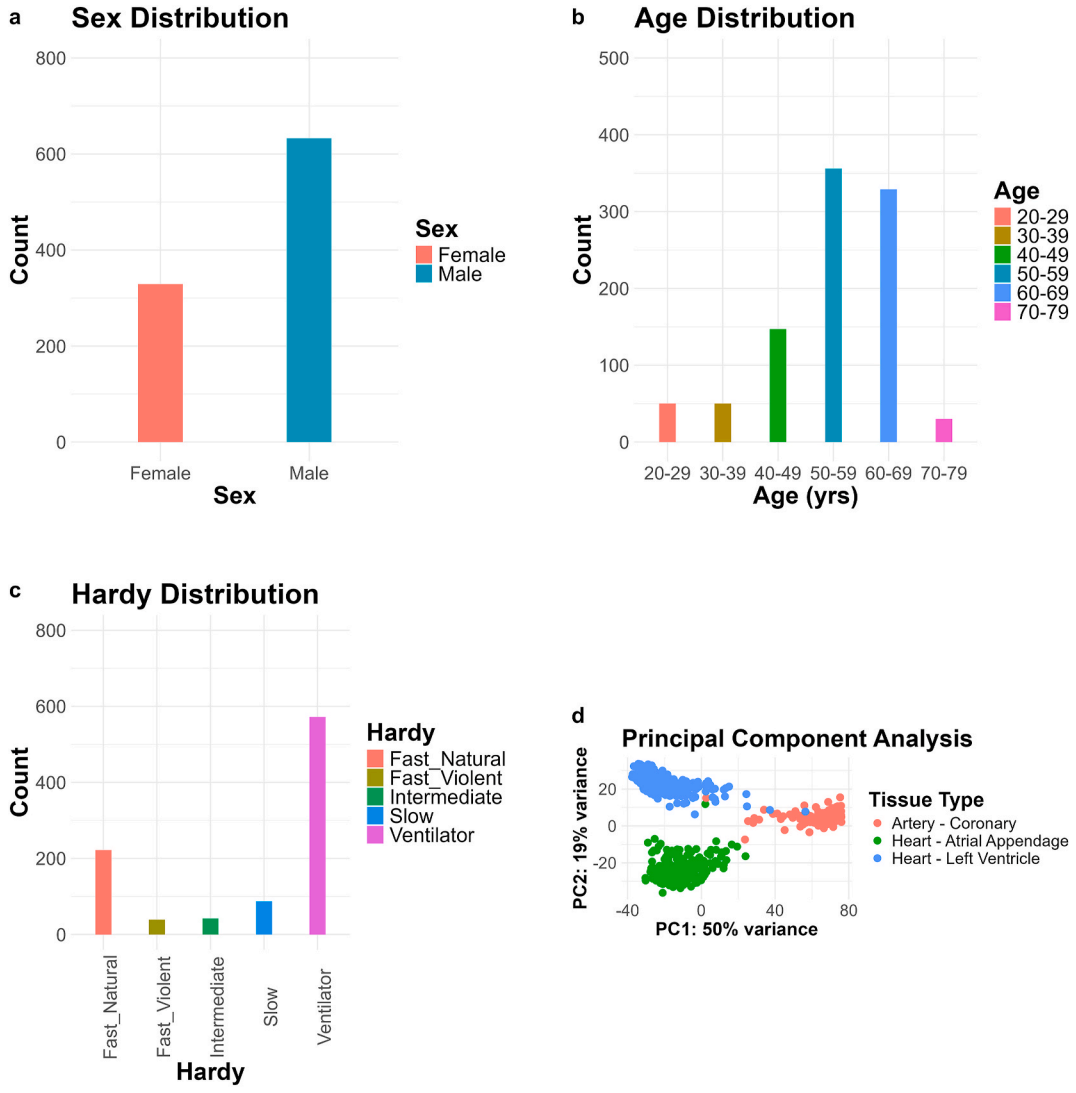

Fig. 1. Descriptive Analysis
a) Sex distribution. b) Age distribution. c) Hardy category distribution. d) Principal component analysis of the grouping variable (SMTSD: Tissue Type).

50, 50, 147, 356, 329, and 30 cases (Fig. 1b). With respect to these age ranges, the atrium, coronary, and ventricle samples accounted for 15, 14, and 21; 17, 12, and 21; 60, 31, and 56; 139, 86, and 131; 146, 59, and 124; as well as 17, 4, and 9 cases, respectively. There were 572 "Ventilator Case", 39 "Violent and fast death", 222 "Fast death of natural causes", 42 "Intermediate death", and 87 "Slow death" cases (Fig. 1c). Each Hardy category comprised 195, 147, and 230; 15, 9, and 15; 119, 30, and 73; 20, 5, and 17; as well as 45, 15, and 27 atrium, coronary, and ventricle samples, respectively. Principal component analysis of SMTSD, revealed reasonable separation (Fig. 1d).

3.2. Bivariate analysis

The tissue type was significantly associated with most of the other variables, including RIN, RNA isolation process and analysis date (Tables 1A and 2A). Significant associations were also demonstrated between RIN and most variables associated with tissue type, including all three demographic factors (Tables 1B and 2B). As a result, the design formula was constructed controlling for RIN, RNA isolation process and analysis date, and all three demographic factors (age, sex, and Hardy scale).

3.3. Overall summary of differentially expressed genes

There were 12656 DEGs as well as 730 and 485 ED-related GO and ASOEA terms respectively, across the three contrasts. Analysis of the atrium vs. coronary (AC) contrast demonstrated 4419 DEGs, with 2626 (59 %) up-regulated. The ventricle vs. coronary (VC) contrast produced 5669 DEGs, 2694 (48 %) being up-regulated, while the atrium vs. ventricle (AV) contrast revealed 2568 DEGs, with 1877 (73 %) up-regulated. Supplementary (Supp) Tables 1–3 contain the complete list of DEGs for each contrast. Functional enrichment analysis identified 253, 328, and 149 GO terms (Supp Tables 4–6) and 260, 177, and 48 ASOEA terms (Supp Tables 7–9) for the AC, VC, and AV contrasts, respectively.

3.4. Atrium vs. coronary (AC) contrast

There was a varied pattern of regulated AC contrast DEGs (Fig. 2a), but more up-regulation, with lack of specific ED-related terms among the top 20 GO terms (Fig. 2b). However, the top 20 ASOEA terms included several membrane integrity-relevant terms ("cell junction" and actin cytoskeleton-related terms) and the lipid metabolism-related term "fatty acid beta-oxidation using acyl-CoA dehydrogenase" (Supp Table 7), while the top clustered ASOEA terms included an immunity/inflammation- and two membrane integrity-related terms (Fig. 2c). The 1122 unique AC contrast DEGs associated with enriched (GO/ASOEA) terms demonstrated a mixed pattern of regulation (Fig. 2d). There were 64 (11 [17.19 %] up-regulated), 122 (47 [38.52 %] up-regulated), 2 (1 [50.00 %] up-regulated), and 16 (4 [25.00 %] up-regulated) DEGs associated with enriched terms, related to immunity/inflammation, membrane integrity, lipid metabolism, and coagulation, respectively (Supp Tables 10–13). There was a pattern of predominant down-regulation within atrial compared to coronary samples among DEGs related to enriched terms linked with immunity/inflammation, membrane integrity, and coagulation (Fig. 3 and Supp Fig. 1).

3.5. Ventricle vs. coronary (VC) contrast

There was an almost even mix of up- and down-regulated VC contrast DEGs (Fig. 4a). The top 20 GO terms included an immunity/inflammation-related term ("adaptive immune response") and a membrane integrity-related term ("cell-cell adhesion via plasma-membrane adhesion molecules") (Fig. 4b), with an immunity/inflammation- and several membrane integrity-related terms among the top 20 ASOEA terms (Supp Table 8) and several membrane integrity-related terms and a lipid metabolism-related term among the top clustered ASOEA terms (Fig. 4c). A total of 1281 unique VC contrast DEGs were associated with enriched terms, and these DEGs demonstrated mostly down-regulation (Fig. 4d). There were 29 (1 [3.45 %] up-regulated), 197 (58 [29.44 %] up-regulated), 5 (2 [40.00 %] up-regulated), and 1 (0 [0.00 %] up-regulated) DEGs associated with enriched terms, related to immunity/inflammation, membrane integrity, lipid metabolism, and coagulation, respectively (Supp Tables 14–17). A predominant down-regulation within ventricle versus coronary samples among the GO/ASOEA shared genes was observed (Fig. 5 and Supp Fig. 2).

3.6. Atrium vs. ventricle (AV) contrast

AV contrast DEGs demonstrated mostly up-regulation (Fig. 6a). Among the top 20 GO terms was a membrane integrity-related term, "cell-cell adhesion via plasma-membrane adhesion molecules" (Fig. 6b), with several membrane integrity-related terms and a lipid metabolism-related term among the top 20 ASOEA terms (Supp Table 9) and membrane integrity-related terms after clustering (Fig. 6c). There were 206 unique AV contrast DEGs associated with enriched terms, with DEGs also exhibiting mostly up-regulation (Fig. 6d). However, the differences were less pronounced compared with the AC and VC contrasts (Fig. 2d

Table 1
Association between SMTSD/SMRIN and categorical variables.

A. SMTSD vs categorical variables (Fisher exact test)		B. SMRIN vs categorical variables (ANOVA or *t*-test)					
Variable [25,26] [a]	p (unadjusted)	Variable [25,26] [a]	df	SumSq	MeanSq	F/t	p (unadjusted)
SMATSSCR	0.340	SMATSSCR	1	26.08	26.08	35.28	**0.000**
SMCENTER	0.050	SMCENTER	2	43.54	21.77	30.16	**0.000**
SMPTHNTS	**0.000**	SMPTHNTS	791	629.25	0.80	1.27	**0.030**
SMUBRID	**0.000**	SMUBRID	2	16.51	8.26	11.01	**0.000**
SMNABTCH	1.000	SMNABTCH	314	269.00	0.86	1.19	**0.040**
SMNABTCHT	**0.000**	SMNABTCHT (t)	960			−6.16	**0.000**
SMNABTCHD	1.000	SMNABTCHD	260	229.07	0.88	1.22	**0.020**
SMGEBTCH	**0.000**	SMGEBTCH	239	266.82	1.12	1.72	**0.000**
SMGEBTCHD	**0.000**	SMGEBTCHD	170	201.93	1.19	1.76	**0.000**
SEX	**0.040**	SEX (wt)	626.32			3.57	**0.000**
AGE	0.330	AGE	5	36.20	7.24	9.89	**0.000**
DTHHRDY	**0.000**	DTHHRDY	4	194.12	48.53	85.74	**0.000**

Bold = significant.
Underline = *t*-test.
Full variable descriptions are available at https://gtexportal.org/home/downloads/adult-gtex/metadata, under "GTEx Analysis V8." [25,26].
[a] SMTSD = Tissue Type; SMRIN = RNA integrity number; SMATSSCR = Autolysis Score; SMCENTER = Collection site; SMPTHNTS = Pathology notes; SMUBRID = Uberon ID; SMNABTCH = Isolation Batch ID; SMNABTCHT = Type of isolation; t = Two Sample *t*-test; SMNABTCHD = Isolation date; SMGEBTCH = Genotype/Expression Batch ID; SMGEBTCHD = Genotype/Expression Batch ID date; wt = Welch Two Sample *t*-test; DTHHRDY = Hardy Scale.

Table 2
Association between SMTSD/SMRIN and numeric factors.

A. SMTSD vs numeric factors (ANOVA)

Variable [25,26] [a]	df	SumSq	MeanSq	F	p (unadjusted)
SMRIN	2	16.51	8.26	11.01	**0.000**
SMTSISCH	2	5719136.74	2859568.37	19.67	**0.000**
SMTSPAX	2	139497.04	69748.52	0.82	0.440
SME2MPRT	2	0.12	0.06	17.62	**0.000**
SMCHMPRS	2	83541621285.94	41770810642.97	0.49	0.610
SMNTRART	2	0.01	0.01	75.19	**0.000**
SMMAPRT	2	0.12	0.06	17.94	**0.000**
SMEXNCRT	2	0.21	0.11	130.57	**0.000**
SMGNSDTC	2	538020412.19	269010206.10	199.67	**0.000**
SMUNMPRT	2	0.00	0.00	0.72	0.490
SMRDLGTH	2	0.00	0.00	0.72	0.490
SME1MMRT	2	0.00	0.00	1.92	0.150
SMSFLGTH	2	555750.35	277875.18	43.23	**0.000**
SMMPPD	2	7337952499635950.00	3668976249817970.00	5.71	**0.000**
SMNTERRT	2	0.01	0.01	72.96	**0.000**
SMRRNANM	2	992273094399997.00	496136547199998.00	251.92	**0.000**
SMRDTTL	2	13752622545879600.00	6876311272939830.00	10.70	**0.000**
SMVQCFL	2	390237615184060.00	195118807592030.00	8.26	**0.000**
SMTRSCPT	2	543478727.60	271739363.80	199.29	**0.000**
SMMPPDPR	2	1834521704975620.00	917260852487812.00	5.76	**0.000**
SMNTRNRT	2	0.14	0.07	108.27	**0.000**
SMMPUNRT	2	0.12	0.06	17.94	**0.000**
SMEXPEFF	2	0.03	0.02	5.08	**0.010**
SMMPPDUN	2	7337952499635950.00	3668976249817970.00	5.71	**0.000**
SME2MMRT	2	0.00	0.00	12.28	**0.000**
SME2ANTI	2	501680926524738.00	250840463262369.00	8.42	**0.000**
SMALTALG	2	22632157803333900.00	11316078901666900.00	71.90	**0.000**
SME2SNSE	2	538196044017094.00	269098022008547.00	8.76	**0.000**
SMMFLGTH	2	598991.79	299495.90	60.47	**0.000**
SME1ANTI	2	510533314985927.00	255266657492963.00	8.35	**0.000**
SMSPLTRD	2	816565271758033.00	408282635879016.00	15.61	**0.000**
SMBSMMRT	2	0.00	0.00	7.12	**0.000**
SME1SNSE	2	524000659846678.00	262000329923339.00	8.63	**0.000**
SME1PCTS	2	0.26	0.13	0.72	0.490
SMRRNART	2	0.11	0.06	272.41	**0.000**
SME1MPRT	2	0.12	0.06	18.18	**0.000**
SME2PCTS	2	0.93	0.46	3.91	**0.020**

B. SMRIN vs numeric factors (Pearson correlation)

Variable [25,26] [a]	t	df	rho	lower_CI	upper_CI	p (unadjusted)
SMTSISCH	−18.56	960	−0.51	−0.56	−0.47	**0.000**
SMTSPAX	−2.13	957	−0.07	−0.13	−0.01	**0.030**
SME2MPRT	−0.82	960	−0.03	−0.09	0.04	0.410
SMCHMPRS	3.91	960	0.13	0.06	0.19	**0.000**
SMNTRART	3.66	960	0.12	0.05	0.18	**0.000**
SMMAPRT	−0.89	960	−0.03	−0.09	0.03	0.370
SMEXNCRT	13.00	960	0.39	0.33	0.44	**0.000**
SMGNSDTC	−2.08	960	−0.07	−0.13	0.00	**0.040**
SME1MMRT	−3.02	960	−0.10	−0.16	−0.03	**0.000**
SMSFLGTH	3.77	960	0.12	0.06	0.18	**0.000**
SMMPPD	6.26	960	0.20	0.14	0.26	**0.000**
SMNTERRT	−3.77	960	−0.12	−0.18	−0.06	**0.000**
SMRRNANM	−6.49	960	−0.21	−0.26	−0.14	**0.000**
SMRDTTL	6.63	960	0.21	0.15	0.27	**0.000**
SMVQCFL	2.69	960	0.09	0.02	0.15	**0.010**
SMTRSCPT	−2.10	960	−0.07	−0.13	0.00	**0.040**
SMMPPDPR	6.27	960	0.20	0.14	0.26	**0.000**
SMNTRNRT	−13.86	960	−0.41	−0.46	−0.35	**0.000**
SMMPUNRT	−0.89	960	−0.03	−0.09	0.03	0.370
SMEXPEFF	6.18	960	0.20	0.13	0.26	**0.000**
SMMPPDUN	6.26	960	0.20	0.14	0.26	**0.000**
SME2MMRT	0.22	960	0.01	−0.06	0.07	0.830
SME2ANTI	6.08	960	0.19	0.13	0.25	**0.000**
SMALTALG	0.91	960	0.03	−0.03	0.09	0.360
SME2SNSE	6.05	960	0.19	0.13	0.25	**0.000**
SMMFLGTH	3.65	960	0.12	0.05	0.18	**0.000**
SME1ANTI	5.94	960	0.19	0.13	0.25	**0.000**
SMSPLTRD	13.98	960	0.41	0.36	0.46	**0.000**
SMBSMMRT	−0.84	960	−0.03	−0.09	0.04	0.400

(*continued on next page*)

Table 2 (*continued*)

B. SMRIN vs numeric factors (Pearson correlation)						
Variable [25,26] [a]	t	df	rho	lower_CI	upper_CI	p (unadjusted)
SME1SNSE	6.15	960	0.19	0.13	0.25	**0.000**
SME1PCTS	2.29	960	0.07	0.01	0.14	**0.020**
SMRRNART	−9.52	960	−0.29	−0.35	−0.23	**0.000**
SME1MPRT	−0.97	960	−0.03	−0.09	0.03	0.330
SME2PCTS	0.24	960	0.01	−0.06	0.07	0.810

Bold = significant.
Underline = Associated with SMTSD but not SMRIN.
Full variable descriptions are available at https://gtexportal.org/home/downloads/adult-gtex/metadata, under "GTEx Analysis V8." [25,26].
[a] SMTSD = Tissue Type; SMRIN = RNA integrity number; SMTSISCH = Total Ischemic time; SMTSPAX = PAXgene fixative time; SME2MPRT = Rate (End 2 Mapping); SMCHMPRS = Chimeric Pairs; SMNTRART = Rate (Intragenic); SMMAPRT = Rate (Mapping); SMEXNCRT = Rate (Exonic); SMGNSDTC = Genes Detected (≥5 exon mapping reads); SMUNMPRT = Rate (Unique Mapped); SMRDLGTH = Read Length (maximum); SME1MMRT = Rate (End 1 Mismatch); SMSFLGTH = Fragment Length StdDev; SMMPPD = Mapped; SMNTERRT = Rate (Intergenic); SMRRNANM = Reads aligned to rRNA regions; SMRDTTL = Total reads; SMVQCFL = Failed QC Check; SMTRSCPT = Transcripts Detected; SMMPPDPR = Mapped Pairs; SMNTRNRT = Rate (Intronic); SMMPUNRT = Unique Mapped Rate of Total; SMEXPEFF = Expression Profiling Efficiency; SMMPPDUN = Unique Mapped; SME2MMRT = Rate (End 2 Mismatch); SME2ANTI = End 2 Antisense; SMALTALG = Alternative Alignments; SME2SNSE = End 2 Sense; SMMFLGTH = Mean Fragment Length; SME1ANTI = End 1 Antisense; SMSPLTRD = Split Reads; SMBSMMRT = Rate (Base Mismatch); SME1SNSE = End 1 Sense; SME1PCTS = End 1 % Sense; SMRRNART = Rate (rRNA); SME1MPRT = Rate (End 1 Mapping); SME2PCTS = End 2 % Sense.

Table 3
Top up-regulated genes for each contrast and category.

AC_ImIn	VC_ImIn	AV_ImIn	AC_Memb	VC_Memb	AV_Memb	AC_Lip	VC_Lip	AV_Lip	AC_Coag
PRKCZ	VEGFA	MS4A1	ACTN2	ACTN2[a]	CLDN18	VLDLR	CD36[a]	STAB2	F8
C6			POF1B	PKP2[a]	FLRT2		VLDLR[a]		F7
TRAC			PKP2	APOA1	CADM3				CD36
VEGFA			DSP	DSP[a]	PTK7				ADAMTS13
COLEC11			ADAM11	CXADR[a]	EPB41L3				
log2 fold change (mean, lowest, and highest) [b]									
2.065562	1.861999	1.488613	2.293720	2.442698	1.724044	1.864702	2.439650	1.862335	1.508999
1.057982	1.861999	1.488613	1.034544	1.002630	1.122959	1.864702	2.124656	1.862335	1.090735
3.635716	1.861999	1.488613	4.719427	5.399410	2.694127	1.864702	2.754643	1.862335	1.769785

AC = Atrium vs. Coronary contrast; AV = Atrium vs. Ventricle contrast; Coag = genes related to coagulation associated with enriched (GO/ASOEA) terms; ImIn = genes related to immunity/inflammation associated with enriched terms; Lip = genes related to lipid metabolism associated with enriched terms; Memb = genes related to membrane integrity associated with enriched terms; VC = Ventricle vs. Coronary contrast.
[a] Genes for which the right ventricle expression score reported in Bgee database [44] used for validation.
[b] Log^2 fold change (mean, lowest, and highest) for each contrast and category.

and 4d). There were only 1 (1 [100.00 %] up-regulated), 9 (7 [77.78 %] up-regulated), 2 (1 [50.00 %] up-regulated), and 0 (0 [0.00 %] up-regulated) DEGs associated with enriched terms, related to immunity/inflammation, membrane integrity, and lipid metabolism, respectively (Supp Tables 18–20). These genes demonstrated predominantly up-regulation, but with milder changes (Fig. 7 and Supp Fig. 3).

3.7. Validation

3.7.1. Enrichment term categorization

The validity of enrichment term categorization was examined by contrasting categorized DEGs with listings of related gene symbols and aliases. There were 105172, 98831, 93272, and 82143 genes/aliases related to "inflammation," "edema" (impaired membrane integrity proxy), "dyslipidemias," and "blood coagulation disorders" respectively, and 100 % of DEGs for each category were found in their corresponding list. This finding lends support for categorization of GO/ASOEA terms.

3.7.2. Verification of expression patterns

Comparisons were also made between the relative expression of the top 5 regulated genes (or less if < 5) in each contrast and category, and relative *Homo sapiens* tissue expression patterns reported in the Bgee database [44]. The top up-regulated DEGs (See Supp Table 21 for complete list – n = 133) as well as the mean, lower, and upper range of the log^2 fold change for all up-regulated DEGs, for each contrast and category, are shown in Table 3. This analysis revealed that AC contrast DEGs were more highly expressed in the right atrium auricular region than left or right coronary arteries. VC contrast DEGs were more highly expressed in the left ventricle (or right ventricle if left ventricle expression was not documented) than left or right coronary arteries. Likewise, AV contrast DEGs were more highly expressed in the right atrium auricular region than left ventricle.

The top down-regulated DEGs (See Supp Table 22 for complete list – n = 315) as well as the mean, lower, and upper range of the log^2 fold change for all down-regulated DEGs, for each contrast and category, are shown in Table 4. AC contrast DEGs were more lowly expressed in the right atrium auricular region than left or right coronary arteries. VC contrast DEGs were also more lowly expressed in the left ventricle than left or right coronary arteries. Finally, AV contrast DEGs were more lowly expressed in the right atrium auricular region than left ventricle (or right ventricle if left ventricle expression was not documented).

3.8. Transcriptional relationship between tissues

Comparisons were made of the DEGs associated with GO/ASOEA terms across each contrast and category. There was only one DEG shared between the AC and VC contrast pair among the immunity/inflammation- and lipid metabolism-related up-regulated genes, with no DEGs between the AC/AV, and VC/AV pairs. With respect to membrane integrity-related DEGs, 33, 2, and 0 genes were common between AC/VC, AC/AV, and VC/AV pairs, respectively. There were only AC contrast coagulation-related DEGs, hence no comparison was possible. Eighteen

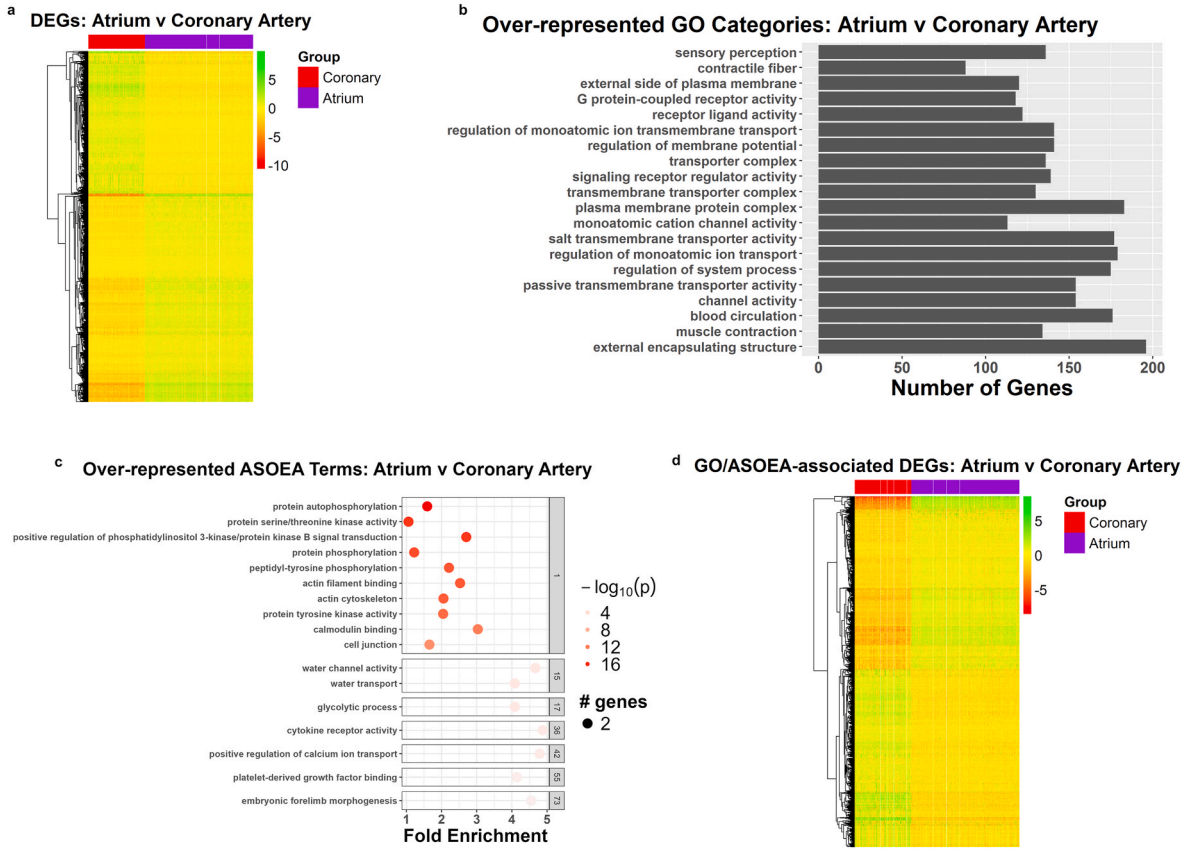

Fig. 2. AC contrast DEGs: Heatmaps of contrast DEGs and associated enrichment terms
a) Heatmap of 4419 AC contrast DEGs. b) Top 20 GO terms. c) Top clustered ASOEA terms. d) Heatmap of 1122 AC contrast DEGs associated with both enriched GO and ASOEA terms.
AC = atrium vs. coronary; DEGs = differentially expressed genes; GO = gene ontology; ASOEA = active-subnetwork-oriented enrichment analysis.

DEGs were shared between the AC and VC contrast pair, for immunity/inflammation-related down-regulated genes. Among membrane integrity- and lipid metabolism-related DEGs, 67, 0, and 0, as well as 1, 0, and 0 were common between the AC/VC, AC/AV, and VC/AV pairs, respectively. Finally, only one coagulation-related DEG was common between the AC/VC pair, with none between the AC/AV, and VC/AV pairs. These findings confirm that, unlike the AC/VC contrast pair, there was almost no overlap between the AC/AV, and VC/AV contrast pairs, and implies substantial similarity in the expression pattern of ED-related genes between atrium and ventricle, as opposed to the coronary artery.

3.9. Pathway analysis

KEGG pathway analysis identified 6, 2, and 0, as well as 0, 0, and 0 ED-related significantly down- and up-regulated pathways (FDR of <0.05) associated with the AC, VC, and AV contrast-associated DEGs respectively, when the "same.dir" parameter was set to "True". There were no identified pathways when "same.dir" was set to "False", which tests for genes not coregulated [45]. The complete lists are provided in Supp Tables 23–25.

Relevant down-regulated pathways associated with the AC contrast included the membrane integrity-related pathway "Cell adhesion molecules," as well as the inflammation/immunity related pathways "Chemokine signaling pathway," "Leukocyte transendothelial migration," "Antigen processing and presentation," "Phagosome," and "Natural killer cell mediated cytotoxicity." Several down-regulated AC contrast-associated DEGs common to GO and ASOEA terms (Supp Table 22), with potential to modulate ED-related processes, were identified among these down-regulated KEGG pathways. These included JAK2 and the chemokine receptor CCR2 (KEGG: Chemokine signaling pathway, Fig. 8a); the cluster of differentiation antigens (CD2, CD6, CD28, PTPRC [CD45] [48], CD80, CD86, VCAM1 [CD106] [49], and ALCAM [CD166] [50]), CD40L [CD40LG], integrins (ITGA4, ITGB1, ITGB2), and CTLA4 (KEGG: Cell Adhesion Molecules: Immune System section, Fig. 9a); the cell adhesion molecule (CAM) VCAM1, α-actinins (ACTN1 and ACTN4), the actin ACTB, integrins (ITGA4, ITGB1, ITGB2), and Thy1 (KEGG: Leukocyte transendothelial migration, Fig. 10); various integrins (ITGB1, ITGB2, ITGB3, and ITGB5) involved in phagocytosis (KEGG: Phagosome, Supp Fig. 4a); and the activating receptor ITGB2, as well as LAT, SYK, and FCER1G (KEGG: Natural killer cell mediated cytotoxicity, Supp Fig. 4b). Down regulation of these genes in the atrium relative to the coronary arteries, including cell adhesion molecules e.g., VCAM1 and various integrins, as well as those related to inflammation/immunity pathways e.g., CCR2 and CD40L, could potentially suppress atherogenesis in the atrium by moderating leukocyte recruitment, trans-endothelial/trans-endocardial migration (LTetM/LTecM), and subsequent inflammation [1,3]. Only one up-regulated AC contrast-associated DEG common to GO and ASOEA terms (Supp Table 21) was identified among down-regulated KEGG pathways: the cluster of differentiation antigen CD36, which is one of several scavenger receptors associated with phagocytosis (KEGG: Phagosome, Supp Fig. 4a). None of the AC contrast-associated DEGs common to GO and ASOEA terms, were identified among the down-regulated KEGG pathway "Antigen processing and presentation."

The VC contrast was associated with down-regulated "Cell adhesion molecules" and "Chemokine signaling pathway" KEGG pathways. There were several down-regulated VC contrast-associated DEGs common to GO and ASOEA terms (Supp Table 22), with potential to modulate ED-

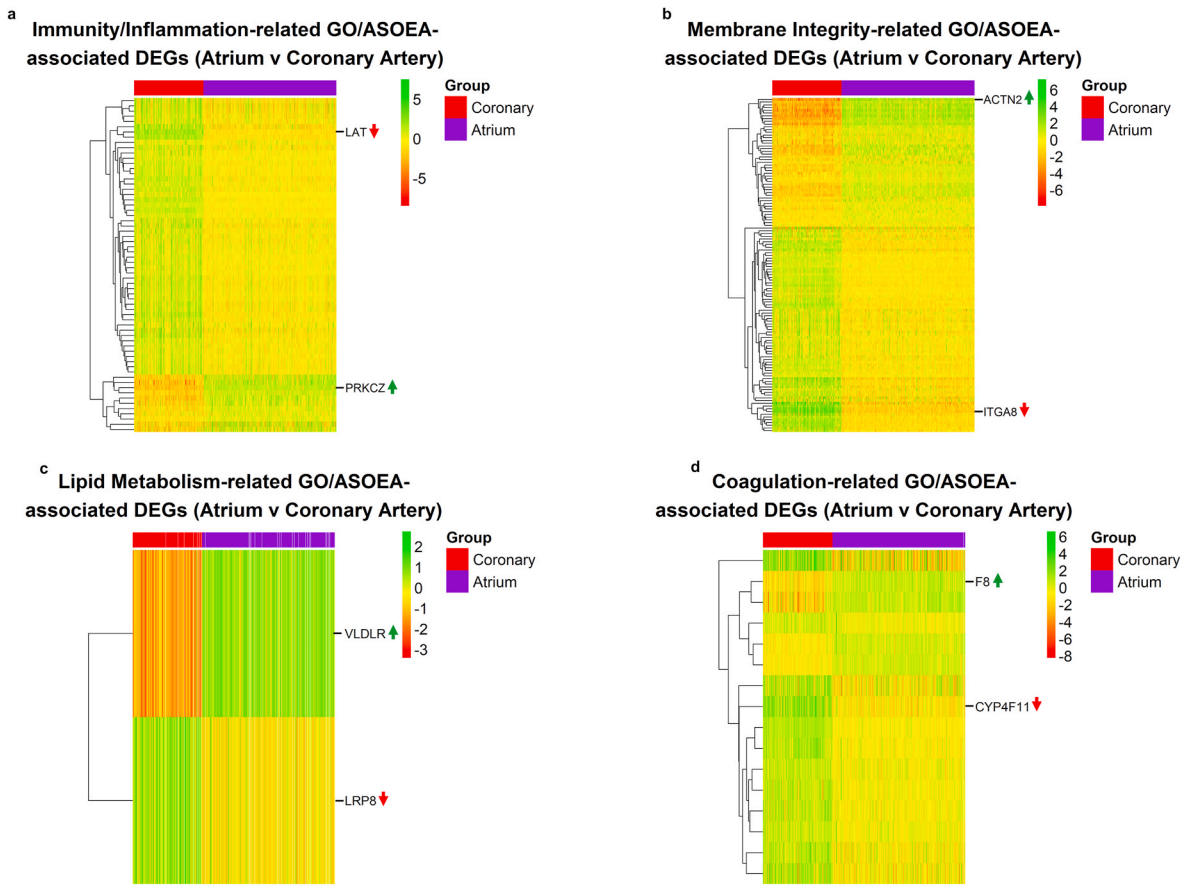

Fig. 3. AC contrast: Endothelial dysfunction-related DEGs
Heatmaps of AC contrast DEGs associated with both enriched GO and ASOEA terms that are related to a) immunity/inflammation, b) membrane integrity, c) lipid metabolism, and d) coagulation, with the top up- and down-regulated genes labelled (up and down arrows respectively).
AC = atrium vs. coronary; DEGs = differentially expressed genes; GO = gene ontology; ASOEA = active-subnetwork-oriented enrichment analysis.

related processes, identified among these down-regulated KEGG pathways. These included JAK2, TIAM1 and the chemokine receptor CCR2 (KEGG: Chemokine signaling pathway, Fig. 8b); and cluster of differentiation antigens (CD2, CD6, PTPRC [CD45] [48], VCAM1 [CD106] [49], and ALCAM [CD166] [50]), CD40LG, integrins (ITGA4, ITGAL, ITGAM, ITGB1, ITGB2, and ITGB7), and SELP (KEGG: Cell Adhesion Molecules: Immune System section, Fig. 9b). As with the AC contrast, down regulation of these genes in the ventricle relative to the coronary arteries, including cell adhesion molecules e.g., VCAM1, SELP, and various integrins, as well as the inflammation/immunity related gene CCR2, could potentially suppress atherogenesis in the ventricle by moderating leukocyte recruitment, trans-endothelial/trans-endocardial migration (LTetM/LTecM), and subsequent inflammation [1,3]. A few up-regulated VC contrast-associated DEGs common to GO and ASOEA terms (Supp Table 21) were also identified among one of the down-regulated KEGG pathways: the CAMs CDH5 and ICAM2, (KEGG: Cell Adhesion Molecules: Immune System section, Fig. 9b). Up regulation of CDH5, a transmembrane component of adherens junctions (AJs) that is integral to controlling endothelial permeability, could potentially suppress atherogenesis in the ventricle by limiting leukocyte diapedesis and subsequent inflammation [51].

All above pathway-associated down-regulated AC and VC contrast genes were more lowly expressed in the right atrium auricular region and left ventricle respectively than left or right coronary arteries, except for VCAM1 in the VC contrast that was found to be more lowly expressed in the right ventricle than left or right coronary arteries (only right ventricle data was available), as documented in the Bgee database [44]. Similarly, all pathway-associated up-regulated genes in the AC and VC contrasts were more highly expressed in the right atrium auricular region and left ventricle respectively than left or right coronary arteries, as documented in the Bgee database [44].

4. Discussion

This study compared the transcriptomes of grossly normal atheroresistant human atrium and ventricle samples with grossly normal atheroprone coronary arteries. The aim was to demonstrate transcriptomic signatures of atheroresistance in the heart chambers, and identify associated molecular targets whose modulation has the potential to moderate development of arterial LDL-induced monocyte-driven inflammatory response (LIMDIR) and therefore atherogenesis, without compromising postcapillary venular microbe-induced granulocyte-driven inflammatory response (MIGDIR). Potential confounders, including age, sex, and Hardy classification (cause of death), were controlled for, to ensure identified differentially expressed genes and regulated pathways were not influenced by these known risks, and likely reflect transcriptomic differences between the studied tissues within the general population.

There were 315 down-regulated and 133 up-regulated endothelial dysfunction (ED) process-related differentially expressed genes (DEGs) across all contrasts, with similar expression pattern between atrium and ventricle. This study also identified transcriptomic signatures of atheroresistance in the heart chambers, associated with immune cell and associated endothelium functions. Pathway analysis tested for co-regulation of genes within the gene set [45], and identified pathways below an FDR q-value of 0.05 [33] as significantly regulated. However,

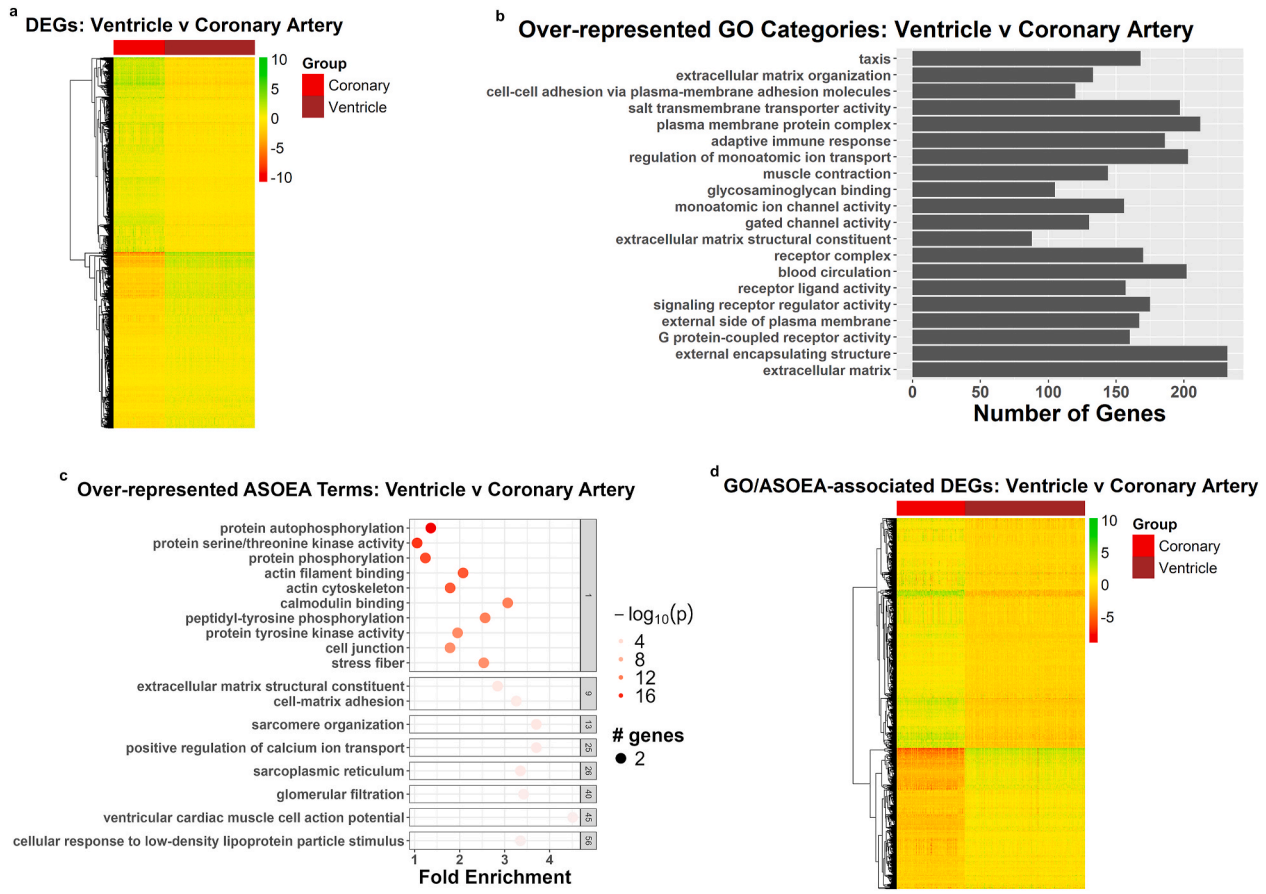

Fig. 4. VC contrast DEGs: Heatmaps of contrast DEGs and associated enrichment terms
a) Heatmap of 5669 VC contrast DEGs. b) Top 20 GO terms. c) Top clustered ASOEA terms. d) Heatmap of 1281 VC contrast DEGs associated with both enriched GO and ASOEA terms.
VC = ventricle vs. coronary; DEGs = differentially expressed genes; GO = gene ontology; ASOEA = active-subnetwork-oriented enrichment analysis.

within the context of divergent cell composition between atrial, ventricular and coronary tissues [52,53], differential gene expression (DGE) could reflect cell-specific expression or average expression across cell types [54]. Accordingly, DGE was interpreted, cognizant of tissue-specific cell composition.

Down-regulated ventricle vs. coronary (VC) contrast DEGs were identified among down-regulated "Chemokine signaling" Kyoto Encyclopedia of Genes and Genomes (KEGG) pathway. The "Chemokine signaling" pathway DEGs included JAK2, TIAM1 and chemokine receptor CCR2. Down-regulated atrium vs. coronary (AC) contrast DEGs identified among the down-regulated "Chemokine signaling" pathway, were JAK2 and CCR2, suggesting similar expression pattern in atrium and ventricle compared with coronary arteries. The tyrosine kinase JAK2 [55] and Rac activator TIAM1 [56] are broadly expressed, making interpretation of their DGE challenging. On the contrary, CCR2 is highly expressed on inflammatory monocytes, with a crucial role in monocyte recruitment into tissues [57]. Given lower heart chamber myeloid cell composition [52,53], down-regulation could reflect the fewer cardiac myeloid cells or cell-specific DGE, which both imply a relatively anti-inflammatory cardiac environment. Additionally, B cell scaffold protein with ankyrin repeats 1 (BANK1), the top down-regulated immunity/inflammation-related VC contrast DEG, was reportedly expressed in B-cells, with known functions including proinflammatory signaling [58]. However, taking into account the lower heart chamber myeloid and lymphoid compositions [52,53], the down-regulation of BANK1 is consistent with recent experimental data derived from single-nucleus RNA sequencing (snRNA-seq) analysis of the entire murine heart that demonstrated prominent BANK1 expression restricted to myeloid and lymphoid cells, most notably monocytes and less so T-cells, with modest average expression in monoblasts and B-cells [59]. In addition, there was weak BANK1 expression in heart chamber-specific cell types including endocardial cells, several cardiomyocyte populations and epicardial-derived fibroblasts, as well as blood vessel-specific/predominant cell types including vascular endothelial cells, smooth muscle cells and endothelial-derived fibroblasts [59]. Together, these findings suggest that down-regulation of BANK1 reflects higher coronary artery myeloid and lymphoid compositions [52,53] and therefore a relatively pro-inflammatory coronary artery environment, consistent with prior analysis that also suggested a relatively pro-inflammatory coronary environment in comparison with the less atheroprone tibial artery [11]. Further, although the role of BANK1 in atherosclerosis is not extensively documented, two recent single-cell RNA sequencing (scRNA-seq) analyses identified B-cells as one immune cell type within atherosclerosis plaques and BANK1 as a B-cell marker [60,61]. However, neither identified this gene as a therapeutic target, suggesting further research is warranted.

A relatively anti-inflammatory cardiac environment was supported by down-regulation of the "Cell Adhesion Molecules: Immune System section" pathway for the VC and AC contrasts. The down-regulated VC contrast DEGs included cluster of differentiation antigens (LFA2 CD2 [62], CD6, PTPRC [CD45] [48], VCAM1 [CD106] [49], and ALCAM [CD166] [50]), CD40LG, integrins (ITGA4, ITGAL, ITGAM, ITGB1, ITGB2, and ITGB7), and SELP. Several of these immune cell-associated molecules have atherogenic potential [50,63–65], including leukocyte-associated CD2 [63], CD6 [50], PTPRC [48], and CD40LG [65] as well as the broadly expressed ALCAM [50]. Also, ITGA4, ITGAL,

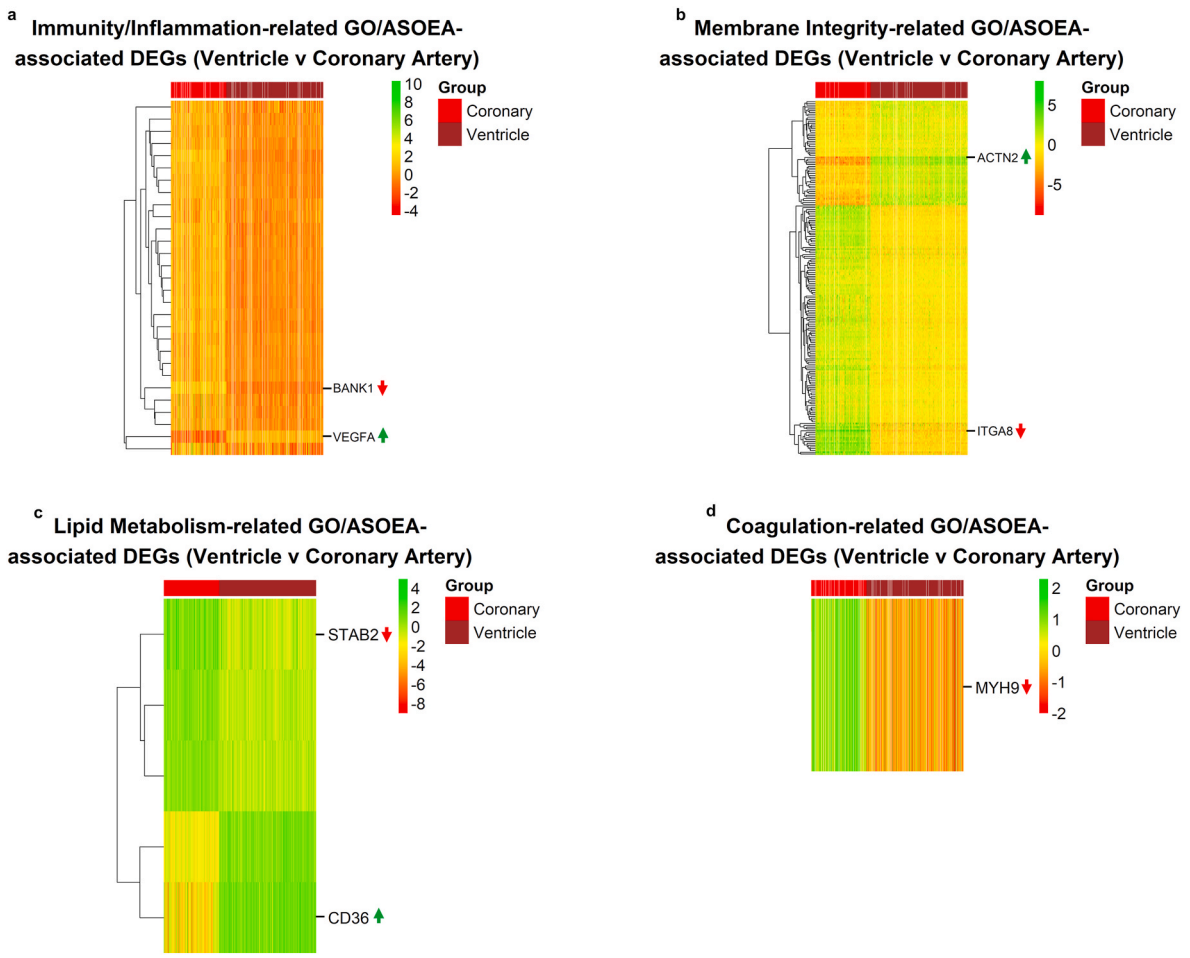

Fig. 5. VC contrast: Endothelial dysfunction-related DEGs
Heatmaps of VC contrast DEGs associated with both enriched GO and ASOEA terms that are related to a) immunity/inflammation, b) membrane integrity, c) lipid metabolism, and d) coagulation, with the top up- and down-regulated genes labelled (up and down arrows respectively).
VC = ventricle vs. coronary; DEGs = differentially expressed genes; GO = gene ontology; ASOEA = active-subnetwork-oriented enrichment analysis.

ITGAM, ITGB1, ITGB2, and ITGB7 are leukocyte integrins, and several are involved in leukocyte interactions with endothelial cell (EC) adhesion molecules, promoting leukocyte recruitment and migration [66–69]. Additional DEGs for the AC contrast were CD28, CD80, CD86 and CTLA4, which are involved in T-cell regulation [70]. Another integrin, ITGA8, the top down-regulated membrane integrity-related DEG for the AC and VC contrasts, is a transmembrane protein expressed by smooth muscle cells [71] with known functions including cell-matrix adhesion [72]. Down-regulated ITGA8 and immune cell-associated cell adhesion molecules (CAMs), could reflect either lower heart chamber SMC and lymphoid composition [52,53] or reduced SMC and leukocyte DGE. However, with respect to ITGA8, its down-regulation is consistent with a recent snRNA-seq analysis of the entire human heart that demonstrated prominent ITGA8 expression only in vascular SMCs [73], suggesting ITGA8 expression reflects the much lower SMC proportion in the heart chamber. Similarly, another snRNA-seq analysis of the entire murine heart also revealed prominent ITGA8 expression only in SMCs, with weak expression in heart chamber-specific cell types including endocardial cells, several cardiomyocyte populations and epicardial-derived fibroblasts, as well as blood vessel-specific cell types including vascular endothelial cells and endothelial-derived fibroblasts [59].

EC-associated down-regulated VC contrast DEGs identified in the "Cell Adhesion Molecules: Immune System section" pathway included vascular cell adhesion molecule 1 (VCAM1) and SELP. VCAM1 was not identified in a previous comparison among major arteries [11], implying utility of comparing atheroresistant heart chambers with atheroprone coronary arteries. VCAM1 expression is primarily in ECs and associated with leukocyte binding [74], resulting in leukocyte recruitment and transendothelial migration [14]. SELP (P-selectin/CD62P) is constitutively expressed on ECs and megakaryocytes and also facilitates leukocyte recruitment during inflammation [75]. The down-regulated AC contrast-associated DEG VCAM1, was also identified among the "Cell Adhesion Molecules" pathway. Considering the higher or similar estimated proportion of ECs in atrial and ventricular tissues respectively, compared with coronary arteries [52,53], down-regulated VCAM1, and possibly SELP, likely reflects cell-specific DGE between heart chamber and coronary ECs. Relative lack of heart chamber EC-associated VCAM1 and SELP could limit leukocyte adhesion to ECs and therefore leukocyte trans-endothelial/trans-endocardial migration (LTetM/LTecM) within atrium and ventricle, suggesting further research is warranted. Down-regulation of VCAM1 is consistent with recent experimental data derived from scRNA-seq analysis of the aging murine heart that demonstrated up-regulation in artery ECs, with greater expression than all other heart chamber-relevant ECs, except for venous capillary ECs (including down-regulation in capillary 1 and lymphatic ECs, as well as neutral expression in capillary 2, arterial capillary, and angiogenic ECs) [76]. Together, these findings suggest that although EC CAMs are primarily expressed in postcapillary venules [15,77], there is a net higher expression of VCAM1 in artery ECs relative to all other EC sub-populations. Further, snRNA-seq analysis of porcine myocardial samples identified a proinflammatory-EC subset, with up-regulation of

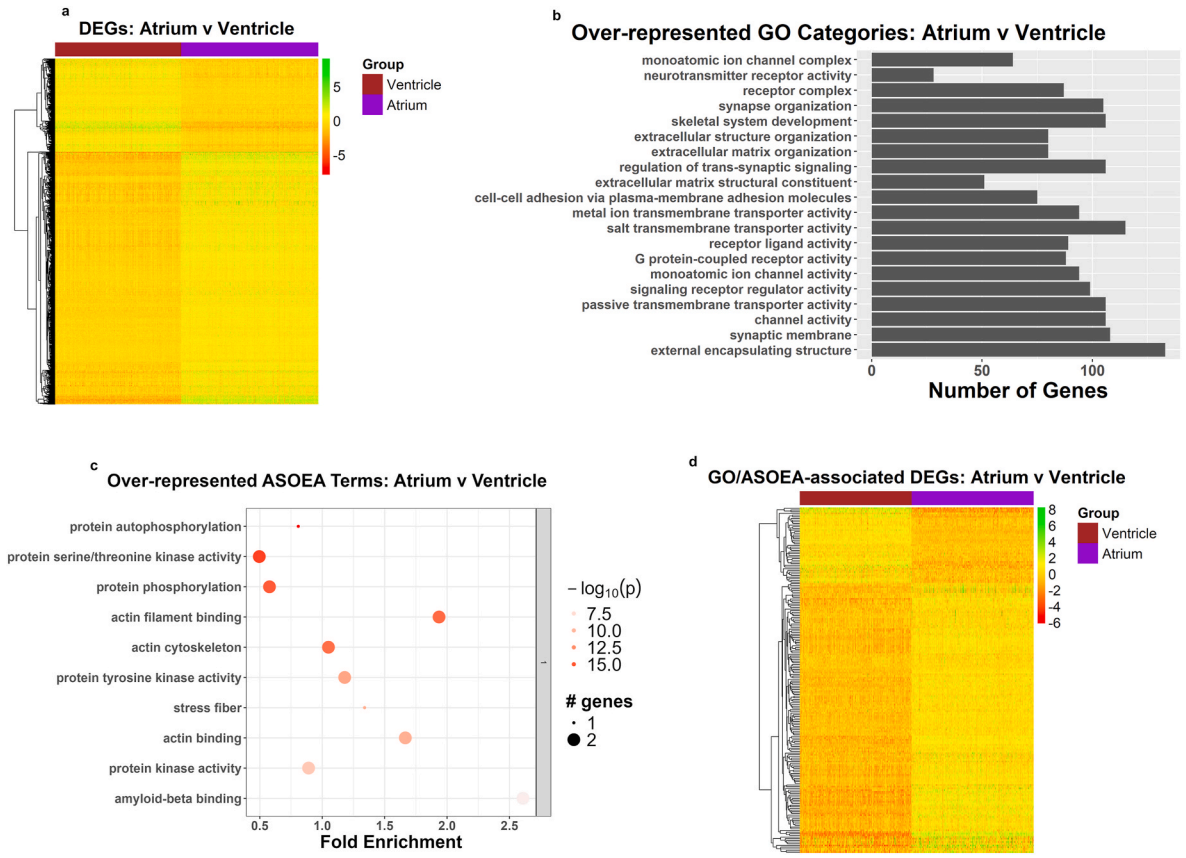

Fig. 6. AV contrast DEGs: Heatmaps of contrast DEGs and associated enrichment terms
a) Heatmap of 2568 AV contrast DEGs. b) Top 20 GO terms. c) Top clustered ASOEA terms. d) Heatmap of 206 AV contrast DEGs associated with both enriched GO and ASOEA terms.
AV = atrium vs. ventricle; DEGs = differentially expressed genes; GO = gene ontology; ASOEA = active-subnetwork-oriented enrichment analysis.

VCAM1 in these ECs from myocardial injury-susceptible transgenic pigs compared with wild type pigs. This subset was associated with enriched GO terms including myeloid leukocyte migration. These findings imply a role for VCAM1 in EC activation and metabolic disease-induced myocardial injury [78]. In addition, the top down-regulated lipid metabolism-related VC contrast DEG, STAB2, is an EC-associated pro-inflammatory scavenger receptor, whose inhibition suppressed patrolling and inflammatory monocytes [79]. STAB2 therefore represents another potential anti-atherosclerosis target [79].

Down-regulated AC contrast-associated DEGs were also identified among three additional down-regulated KEGG pathways related to immunity/inflammation and membrane biology. Various integrins (ITGB1, ITGB2, ITGB3, and ITGB5) were identified among the down-regulated KEGG pathway "Phagosome," with the first two previously identified in the "Cell Adhesion Molecules" pathway. ITGB1, ITGB3, and ITGB5 signaling is associated with endothelial activation, while ITGB1 and ITGB2 promote monocyte recruitment and migration in atherosclerosis [67]. In addition to ITGB2, the DEGs LAT, SYK, and FCER1G were identified in the "Natural killer cell mediated cytotoxicity" KEGG pathway. The tyrosine kinase SYK has wide cell expression including hematopoietic cells and ECs [80], where it functions downstream of the interaction between antigen and fragment crystallizable (FC) receptors [81], with subsequent phosphorylation and activation of downstream signal molecules including LAT [82], the top down-regulated immunity/inflammation-related AC contrast DEG. These results suggest possible reduction in leukocyte recruitment, adhesion, and therefore LTetM/L-TecM, but cell composition differences between samples [52,53], present interpretative challenges. Finally, among the leukocyte trans-endothelial migration (LTetM)-associated DEGs, VCAM1, ITGA4, ITGB1, and ITGB2 were previously identified in the "Cell Adhesion Molecules" pathway. Additional LTetM-associated DEGs were the α-actinins ACTN1 and ACTN4, the actin ACTB (β-actin) and Thy1, which despite potential roles in LTetM [15,69,83], are broadly expressed [83–85], complicating interpretation.

A few up-regulated DEGs were identified among down-regulated KEGG pathways. The AC contrast-associated DEG CD36, was identified among the down-regulated "Phagosome" pathway, and among VC contrast-associated DEGs, the cell adhesion molecules CDH5 and ICAM2, were identified among the down-regulated "Cell Adhesion Molecules" pathway. ICAM2 is an adhesion molecule involved in leukocyte adhesion [86]. The membrane glycoprotein CD36, the top down- and up-regulated lipid metabolism-related atrium vs. ventricle (AV) and VC contrast DEG respectively, has a potential role in atherogenesis by promoting oxLDL uptake by macrophages [87]. However, both demonstrate broad expression [86,87], making interpretation challenging. On the contrary, CDH5 (cadherin 5/vascular endothelial cadherin/VE-cadherin) is specific to vascular and endocardial ECs [88,89], and as the transmembrane component of adherens junctions (AJs) is integral to controlling endothelial permeability and leukocyte diapedesis [51]. Considering the estimated similar proportion of ECs in ventricular and coronary tissues [52,53], ventricular CDH5 up-regulation likely reflects EC-specific DGE and strengthened ventricular AJs. This interpretation finds support from a recent scRNA-seq analysis of the fetal human heart that revealed prominent CDH5 expression was restricted to ECs [90]. However, among the 6 EC sub-populations identified (see Supplementary material), the 2 presumed endocardial EC sub-populations (EC1 and EC2), identified by the mouse endocardium-associated NPR3, demonstrated similar or lower CDH5

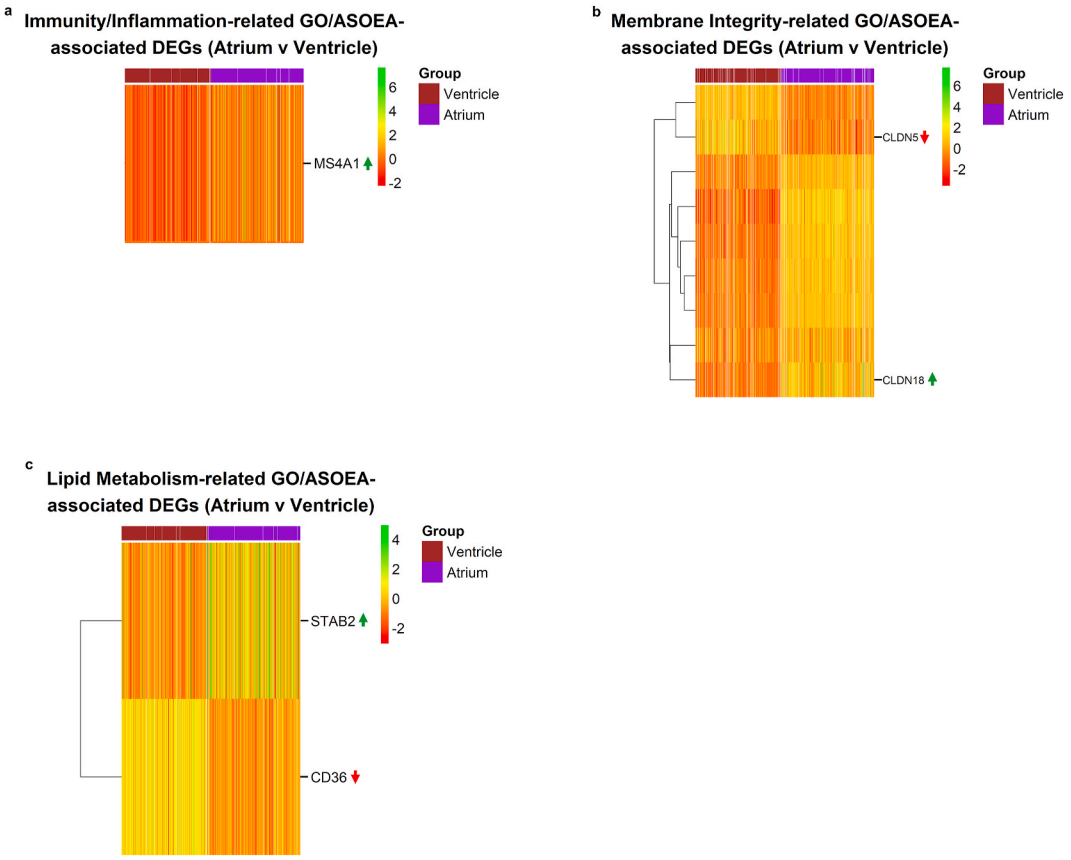

Fig. 7. AV contrast: Endothelial dysfunction-related DEGs
Heatmaps of AV contrast DEGs associated with both enriched GO and ASOEA terms that are related to a) immunity/inflammation, b) membrane integrity, and c) lipid metabolism, with the top up- and down-regulated genes labelled (up and down arrows respectively).
AV = atrium vs. ventricle; DEGs = differentially expressed genes; GO = gene ontology; ASOEA = active-subnetwork-oriented enrichment analysis.

Table 4
Top down-regulated genes for each contrast and category.

AC_ImIn	VC_ImIn	AC_Memb	VC_Memb	AV_Memb	AC_Lip	VC_Lip	AV_Lip	AC_Coag	VC_Coag
LAT	BANK1	ITGA8	ITGA8	CLDN5	LRP8	STAB2	CD36[a]	CYP4F11	MYH9
CLU	IL7	NPNT	SFRP2	PCDH1		SORL1		SERPINE1	
THY1	GREM2	ROBO2	ROBO2			LRP8		ITGB3	
CD28	MS4A1	SFRP2	NPNT					MMRN1	
CD80	CD79A	EDIL3	PPFIA2					MYH9	
log2 fold change (Mean, lowest, and highest) [b]									
−1.406838	−1.671596	−1.879950	−2.089818	−1.401516	−1.014549	−1.473577	−1.204880	−1.607326	−1.440234
−1.019221	−1.014831	−1.001159	−1.002197	−1.153766	−1.014549	−1.046591	−1.204880	−1.034799	−1.440234
−2.754516	−3.557920	−4.755058	−6.110960	−1.649266	−1.014549	−2.176626	−1.204880	−2.989780	−1.440234

AC = Atrium vs. Coronary contrast; AV = Atrium vs. Ventricle contrast; Coag = genes related to coagulation associated with enriched (GO/ASOEA) terms; ImIn = genes related to immunity/inflammation associated with enriched terms; Lip = genes related to lipid metabolism associated with enriched terms; Memb = genes related to membrane integrity associated with enriched terms; VC = Ventricle vs. Coronary contrast.
[a] Genes for which the right ventricle expression score reported in Bgee database [44] used for validation.
[b] Log^2 fold change (mean, lowest, and highest) for each contrast and category.

expression compared with 3 of the other EC sub-populations [90]. This suggest that up-regulation of CDH5 may result primarily from non-endocardial ventricular ECs including capillary and venous ECs [52], which could limit LTetM within the healthy ventricle. This is consistent with the observation that the most prominent CDH5 expression was documented in the EC6 sub-population, the only population with prominent fatty acid binding protein 4 (FABP4) expression [90], a protein immunolocalized in ECs of myocardial capillaries and small veins, but not arterial ECs, within the mouse and human heart [91]. Finally, fibulin 5 (FBLN5) was prominent only in the EC4 sub-population [90], implying arterial lineage [92], whose CDH5 expression was markedly less than in the EC6 sub-population [90], which is consistent with the ventricular CDH5 up-regulation reported here. Further research on the EC sub-population-specific role of CHD5 within the heart, and its potential modulation, appear warranted.

This study therefore identified transcriptomic signatures of atheroresistance in the human atrium and ventricle related to EC and related immune cell functions, that could limit leukocyte recruitment and adhesion to ECs within the atrium and ventricle, as well as enhance AJs within the ventricle. VCAM1 is an adhesion molecule whose expression

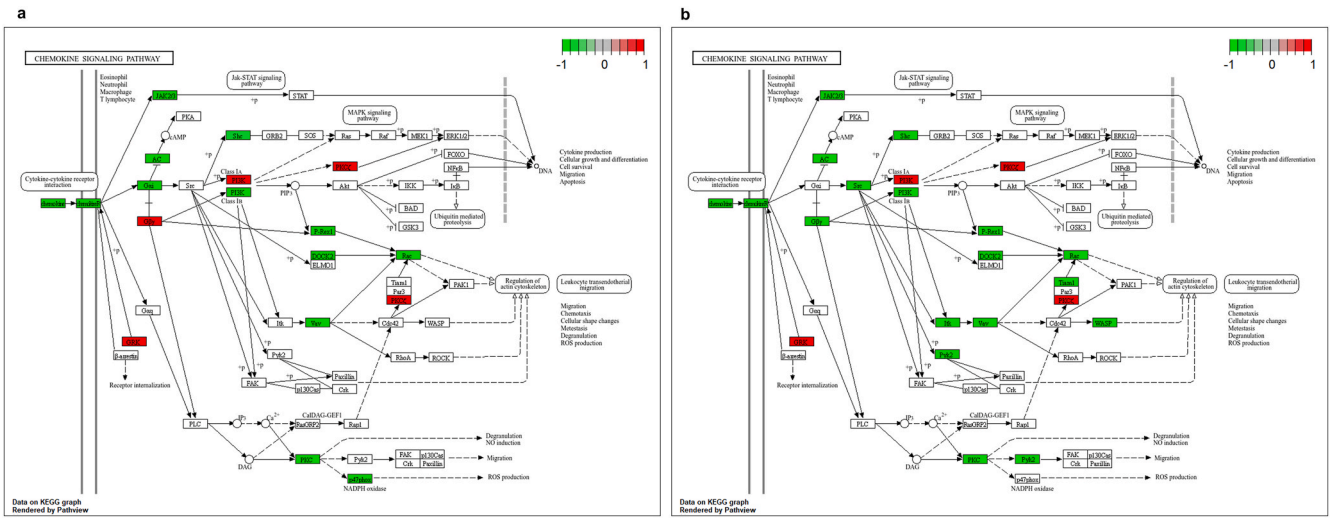

Fig. 8. KEGG "Chemokine signaling" pathway
KEGG "Chemokine signaling" pathway highlighting the associated a) AC and b) VC contrast DEGs. Shading = up- or down-regulation.
KEGG = Kyoto Encyclopedia of Genes and Genomes; AC = atrium vs. coronary; VC = ventricle vs. coronary; DEGs = differentially expressed genes.

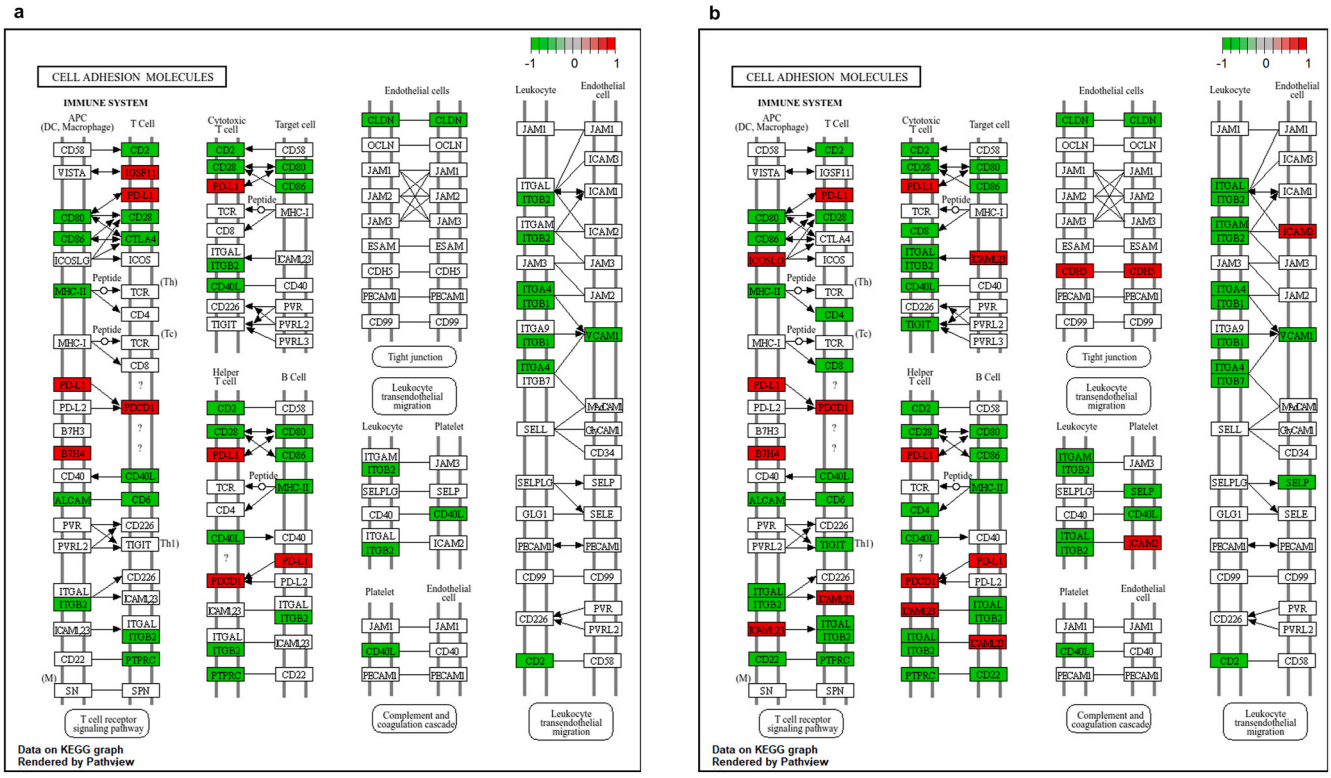

Fig. 9. KEGG "Cell Adhesion Molecules" pathway
KEGG "Cell Adhesion Molecules (Immune System section)" pathway highlighting the associated a) AC and b) VC contrast DEGs. Shading = up- or down-regulation.
KEGG = Kyoto Encyclopedia of Genes and Genomes; AC = atrium vs. coronary; VC = ventricle vs. coronary; DEGs = differentially expressed genes.

is increased on ECs in response to de-novo or oxidized LDL-induced cytokines, which facilitates leukocyte binding [74,93] via VLA-4. This interaction triggers increased EC free calcium and reactive oxygen species that activates myosin light-chain kinase and protein kinase C α, with subsequent phosphorylation of AJ-associated CDH5 and its dissociation from links with the actin cytoskeleton [14,69,94]. The combined effect of activated myosin light-chain kinase-induced contraction of the EC body and weakened AJs, enhances LTetM [14,69], with atherogenic potential [1]. Limited cardiac LTetM could therefore result from reduced leukocyte adhesion [74] via down-regulation of heart chamber EC-associated VCAM1, and strengthened ventricular AJs [51] via EC-associated CDH5 up-regulation, as reported by this study. Reduced LTetM could subsequently limit cardiac inflammation, as reflected by the observed relatively anti-inflammatory heart chamber environment, including down-regulation of the potentially proinflammatory STAB2 [79] and BANK1 [58]. Accordingly, and based on their more straightforward interpretation in this study [52,53], BANK1, STAB2, VCAM1, and CDH5 appear to represent the strongest identified targets for

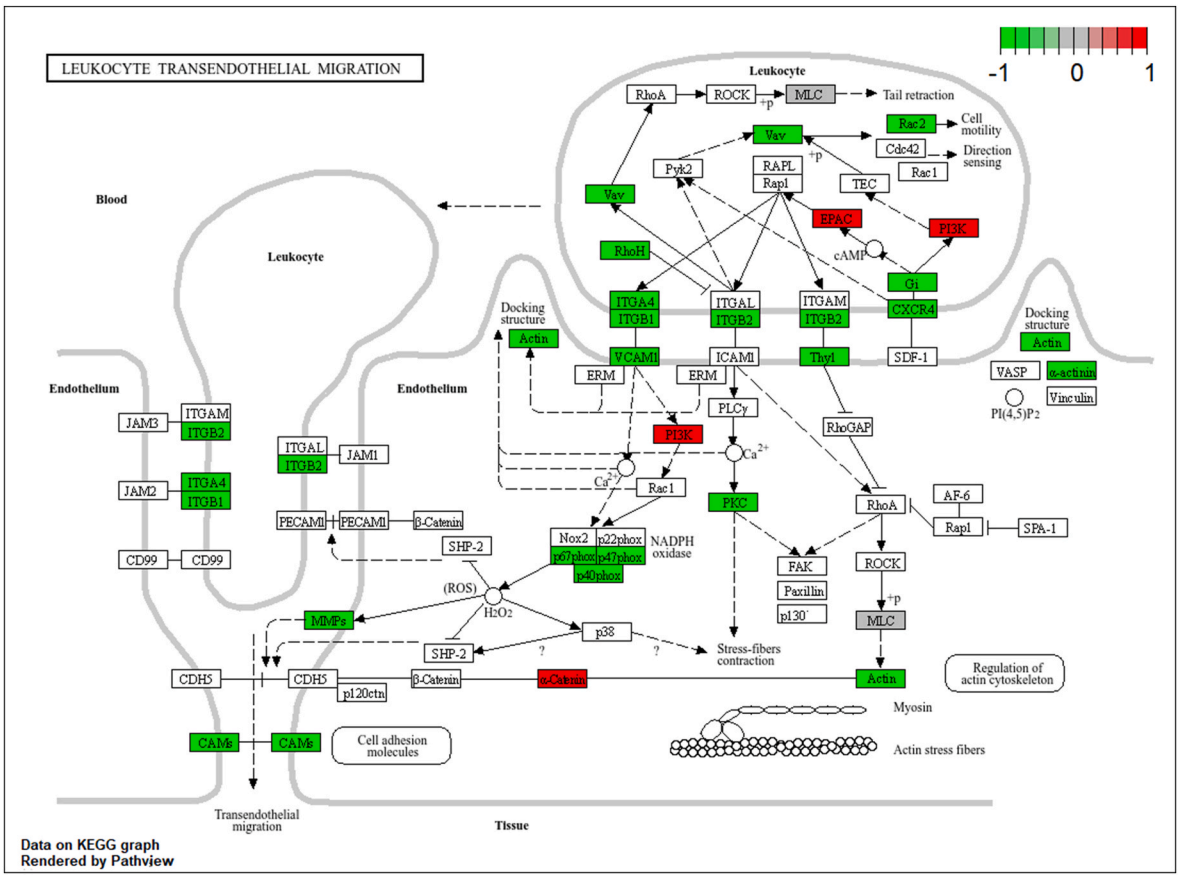

Fig. 10. KEGG "Leukocyte transendothelial migration" pathway
KEGG "Leukocyte transendothelial migration" pathway highlighting the associated AC contrast DEGs. Shading = up- or down-regulation.
KEGG = Kyoto Encyclopedia of Genes and Genomes; AC = atrium vs. coronary; DEGs = differentially expressed genes.

atherosclerosis therapeutics.

Identification of atheroresistance transcriptomic signatures also highlights therapeutic targets applicable to atheroprone regions of the cardiovascular system (CVS). Many potential targets were studied, including CCR2 [95], STAB2 [79], integrins β2, αLβ2, and α4β7 [68], SELP [19], VCAM1, the VLA-4/VCAM1 interaction [16], and CDH5 [96]. However to the best of this authors knowledge, BANK1 has not been specifically investigated. Further, systemic targeting has often proved problematic, including inhibition of inflammatory mediators or EC CAMs that rendered patients immunocompromised [15–19]. On the contrary, targeting specific molecules within a particular cell and tissue context, appears prudent. For example, a recent snRNA-seq analysis of the entire murine heart demonstrated prominent BANK1 expression most notably in monocytes [59], a key cell type involved in atherogenesis [1,3]. Similarly, although there are known interactions involving both VCAM1 and CDH5, with the filamentous (F)-actin cytoskeleton within ECs [69], there is evidence of significantly increased actin protein synthesis in arterial compared with venous ECs, with F-actin microfilaments being scarce or lacking in venous ECs [97], and F-actin reported to end in AJs within arterial ECs, but not venous ECs [98]. Together, these findings suggest new directions for atherosclerosis treatment, including targeting immune cell-associated BANK1 as well as arterial EC-associated VCAM1 and CDH5, aimed at modulating vascular inflammation. Although the American College of Cardiology and American Heart Association do not recommend routine anti-inflammatory therapy for primary prevention of atherosclerotic cardiovascular disease [99], the current findings support continued efforts to develop anti-inflammatory preventative strategies [18]. Admittedly, recent clinical trials involving systemic administration of molecules targeting VCAM1 have been disappointing, due to side effects or poor efficacy, but have encouraged exploring targeted approaches, including nano-formulated drugs [16]. Future research might therefore explore additional novel methods that target artery-specific immune cells and ECs. Such methods could facilitate the use of in-vivo models to study for example, whether targeted inhibition of VCAM1 expressed on atheroprone arteries, limits influx of immune cells and subsequently suppresses vascular inflammation, including reduction in BANK1. Further research might also aim to inhibit BANK1 directly. In addition, over-expressed BANK1 could potentially serve as a diagnostic marker of vascular inflammation, another avenue for investigation.

Among the study strengths, this paper utilized Genotype-Tissue Expression (GTEx) project data that facilitates direct comparison of tissues not normally harvested from the same individual [20]. There were also almost 1000 cases across a wide age range. In addition, this study categorized enrichment terms into ED-related processes, which complemented pathway analysis. However, the GTEx project does not facilitate direct gene expression comparison between cell types [27]. This potential limitation was mitigated by reviewing relevant experimental data. Also, females comprised only approximately a third of cases; hence sex was controlled for in the analysis. Further, because the tissues utilized were grossly normal postmortem samples [21], the gene expression reported may not fully reflect the atherosclerotic state. However, they likely reflect pre-existing transcriptomic differences across normal tissues, consistent with the study aims. In addition, samples involved multiple RNA methodologies and poor tissue quality, which were also controlled for during data analysis.

In conclusion, this study identified transcriptomic signatures of atheroresistance within the atrium and ventricle related to immune cell and associated endothelium functions. To the best of this author's knowledge, this is the first such report. The atheroresistance signatures

highlight potential candidates for targeted atherosclerosis therapeutics, including immune cell-associated BANK1 as well as arterial EC-associated VCAM1 and CDH5, that may not compromise MIGDIR within postcapillary venules.

Consent to participate

Not applicable as this study involved bioinformatic analysis of public data.

Ethical considerations

Not applicable as this study involved bioinformatic analysis of public data.

Consent for publication

Not applicable as this study involved bioinformatic analysis of public data.

Data availability

The project datasets (GTEx Analysis V8: dbGaP accession number phs000424.v8.p2) are publicly available from the GTEx website at https://gtexportal.org/home/downloads/adult-gtex/bulk_tissue_expression, under “GTEx Analysis V8”, “Gene read counts by tissue”.

Funding

This research did not receive any specific grant from funding agencies in the public, commercial, or not-for-profit sectors.

Declaration of competing interest

The authors declare that they have no known competing financial interests or personal relationships that could have appeared to influence the work reported in this paper.

Appendix A. Supplementary data

Supplementary data to this article can be found online at https://doi.org/10.1016/j.bbrep.2025.102007.

References

[1] A.J. Lusis, Atherosclerosis, Nature 407 (2000) 233–241, https://doi.org/10.1038/35025203.
[2] D. Wolf, K. Ley, Immunity and inflammation in atherosclerosis, Circ. Res. 124 (2019) 315–327, https://doi.org/10.1161/circresaha.118.313591.
[3] P. Libby, Interleukin-1 beta as a target for atherosclerosis therapy: biological basis of CANTOS and beyond, J. Am. Coll. Cardiol. 70 (2017) 2278–2289, https://doi.org/10.1016/j.jacc.2017.09.028.
[4] WHO, The Top 10 Causes of Death, World Health Organization, 2020. https://www.who.int/news-room/fact-sheets/detail/the-top-10-causes-of-death. (Accessed 10 August 2023).
[5] L.P. Peng, J. Wen, K. Yang, S.L. Zhao, J. Dai, Z.S. Liang, Y. Cao, Effects of arterial blood on the venous blood vessel wall and differences in percentages of lymphocytes and neutrophils between arterial and venous blood, Medicine (Baltim.) 97 (2018) e11201, https://doi.org/10.1097/md.0000000000011201.
[6] T. Yamaguchi, K. Morino, Perivascular mechanical environment: a narrative review of the role of externally applied mechanical force in the pathogenesis of atherosclerosis, Front. Cardiovasc. Med. 9 (2022), https://doi.org/10.3389/fcvm.2022.944356.
[7] S. Dalager, W.P. Paaske, I.B. Kristensen, J.M. Laurberg, E. Falk, Artery-related differences in atherosclerosis expression, Stroke 38 (2007) 2698–2705, https://doi.org/10.1161/STROKEAHA.107.486480.
[8] M.S. Mohamed-Yassin, N. Baharudin, S. Abdul-Razak, A.S. Ramli, N.M. Lai, Global prevalence of dyslipidaemia in adult populations: a systematic review protocol, BMJ Open 11 (2021) e049662, https://doi.org/10.1136/bmjopen-2021-049662.
[9] N. Lasrado, B. Yalaka, J. Reddy, Triggers of inflammatory heart disease, Front. Cell Dev. Biol. 8 (2020), https://doi.org/10.3389/fcell.2020.00192.
[10] M.J. Tilly, S. Geurts, A.M. Pezzullo, W.M. Bramer, N.M.S. de Groot, M. Kavousi, M. P.M. de Maat, The association of coagulation and atrial fibrillation: a systematic review and meta-analysis, Europace 25 (2023) 28–39, https://doi.org/10.1093/europace/euac130.
[11] P.A. Brown, Genes differentially expressed across major arteries are enriched in endothelial dysfunction-related gene sets: implications for relative inter-artery atherosclerosis risk, Bioinf. Biol. Insights 18 (2024) 11779322241251563, https://doi.org/10.1177/11779322241251563.
[12] T. Örd, T. Lönnberg, V. Nurminen, A. Ravindran, H. Niskanen, M. Kiema, K. Õunap, M. Maria, P.R. Moreau, P.P. Mishra, S. Palani, J. Virta, H. Liljenbäck, E. Aavik, A. Roivainen, S. Ylä-Herttuala, J.P. Laakkonen, T. Lehtimäki, M.U. Kaikkonen, Dissecting the polygenic basis of atherosclerosis via disease-associated cell state signatures, Am. J. Hum. Genet. 110 (2023) 722–740, https://doi.org/10.1016/j.ajhg.2023.03.013.
[13] S. Verma, A. Kumar, R. Narang, A.K. Bisoi, D.K. Mitra, Signature transcriptome analysis of stage specific atherosclerotic plaques of patients, BMC Med. Genom. 15 (2022) 99, https://doi.org/10.1186/s12920-022-01250-8.
[14] W.A. Muller, Mechanisms of leukocyte transendothelial migration, Annu. Rev. Pathol. 6 (2011) 323–344, https://doi.org/10.1146/annurev-pathol-011110-130224.
[15] L. Schimmel, N. Heemskerk, J.D. van Buul, Leukocyte transendothelial migration: a local affair, Small GTPases 8 (2017) 1–15, https://doi.org/10.1080/21541248.2016.1197872.
[16] J.R. Pickett, Y. Wu, L.F. Zacchi, H.T. Ta, Targeting endothelial vascular cell adhesion molecule-1 in atherosclerosis: drug discovery and development of vascular cell adhesion molecule-1-directed novel therapeutics, Cardiovasc. Res. 119 (2023) 2278–2293, https://doi.org/10.1093/cvr/cvad130.
[17] M. Kumric, H. Urlic, J. Bozic, M. Vilovic, T. Ticinovic Kurir, D. Glavas, D. Miric, J. Zanchi, A. Bradaric-Slujo, M. Lozo, J.A. Borovac, Emerging therapies for the treatment of atherosclerotic cardiovascular disease: from bench to bedside, Int. J. Mol. Sci. 24 (2023), https://doi.org/10.3390/ijms24098062.
[18] H. Ait-Oufella, P. Libby, Inflammation and atherosclerosis: prospects for clinical trials, Arterioscler. Thromb. Vasc. Biol. 44 (2024) 1899–1905, https://doi.org/10.1161/ATVBAHA.124.320155.
[19] E. Voutyritsa, G. Kyriakos, A. Patsouras, C. Damaskos, A. Garmpi, E. Diamantis, N. Garmpis, S. Savvanis, Experimental agents for the treatment of atherosclerosis: new directions, J. Exp. Pharmacol. 13 (2021) 161–179, https://doi.org/10.2147/jep.S265642.
[20] L.J. Carithers, K. Ardlie, M. Barcus, P.A. Branton, A. Britton, S.A. Buia, C. C. Compton, D.S. DeLuca, J. Peter-Demchok, E.T. Gelfand, P. Guan, G. E. Korzeniewski, N.C. Lockhart, C.A. Rabiner, A.K. Rao, K.L. Robinson, N.V. Roche, S.J. Sawyer, A.V. Segrè, C.E. Shive, A.M. Smith, L.H. Sobin, A.H. Undale, K. M. Valentino, J. Vaught, T.R. Young, H.M. Moore, A novel approach to high-quality postmortem tissue procurement: the GTEx project, biopreserv, Biobank 13 (2015) 311–319, https://doi.org/10.1089/bio.2015.0032.
[21] GTEx, GTEx tissue harvesting work instruction VER. 03.05. https://biospecimens.cancer.gov/resources/sops/docs/GTEx_SOPs/BBRB-PR-0004-W1%20GTEx%20Tissue%20Harvesting%20Work%20Instruction.pdf. (Accessed 18 July 2023).
[22] Broad Institute of MIT and Harvard, Data from: gene read counts for heart - atrial appendage, GTEx Analysis V8. GTExPortal, https://storage.googleapis.com/adult-gtex/bulk-gex/v8/rna-seq/counts-by-tissue/gene_reads_2017-06-05_v8_heart_atrial_appendage.gct.gz, 2017.
[23] Broad Institute of MIT and Harvard, Data from: gene read counts for artery - coronary, GTEx Analysis V8. GTExPortal, https://storage.googleapis.com/adult-gtex/bulk-gex/v8/rna-seq/counts-by-tissue/gene_reads_2017-06-05_v8_artery_coronary.gct.gz, 2017.
[24] Broad Institute of MIT and Harvard, Data from: gene read counts for heart - left ventricle, GTEx Analysis V8. GTExPortal, https://storage.googleapis.com/adult-gtex/bulk-gex/v8/rna-seq/counts-by-tissue/gene_reads_2017-06-05_v8_heart_left_ventricle.gct.gz, 2017.
[25] Broad Institute of MIT and Harvard. Data from: A data dictionary that describes each column in the GTEx_Analysis_v8_Annotations_SampleAttributesDS.txt. 2017; GTEx Analysis V8. GTExPortal. https://storage.googleapis.com/adult-gtex/annotations/v8/metadata-files/GTEx_Analysis_v8_Annotations_SampleAttributesDD.xlsx.
[26] Broad Institute of MIT and Harvard. Data from: A data dictionary that describes each column in the GTEx_Analysis_v8_Annotations_SubjectPhenotypesDS.txt. 2017; GTEx Analysis V8. GTExPortal. https://storage.googleapis.com/adult-gtex/annotations/v8/metadata-files/GTEx_Analysis_v8_Annotations_SubjectPhenotypesDD.xlsx.
[27] GTEx, Laboratory methods. https://gtexportal.org/home/methods, 2019. (Accessed 18 July 2023).
[28] Illumina, TruSeq™ RNA and DNA library preparation kits v2. http://www.illumina.com/documents/products/datasheets/datasheet_truseq_sample_prep_kits.pdf, 2014. (Accessed 18 July 2023).
[29] T. Natoli, CMap tools in R, Bioconductor (2023). https://bioconductor.org/packages/release/bioc/html/cmapR.html. (Accessed 18 July 2023).
[30] M. Carlson, Genome wide annotation for Human, Bioconductor (2019). http://bioconductor.org/packages/release/data/annotation/html/org.Hs.eg.db.html. (Accessed 18 July 2023).
[31] M. Morgan, V. Obenchain, J. Hester, H. Pagès, SummarizedExperiment container, Bioconductor (2023). https://bioconductor.org/packages/release/bioc/html/SummarizedExperiment.html. (Accessed 18 July 2023).
[32] M.I. Love, W. Huber, S. Anders, Moderated estimation of fold change and dispersion for RNA-seq data with DESeq2, Genome Biol. 15 (2014) 550, https://doi.org/10.1186/s13059-014-0550-8.

[33] Y. Benjamini, Y. Hochberg, Controlling the false discovery rate: a practical and powerful approach to multiple testing, J. R Stat Soc. Series B Methodol. 57 (1995) 289–300, https://doi.org/10.1111/j.2517-6161.1995.tb02031.x.
[34] R. Kolde pheatmap, RDocumentation (2019), version 1.0.12. https://www.rdocumentation.org/packages/pheatmap/versions/1.0.12. (Accessed 18 July 2023).
[35] G. Yu, L.-G. Wang, Y. Han, Q.-Y. He, clusterProfiler: an R Package for comparing biological themes among gene clusters, OMICS 16 (2012) 284–287, https://doi.org/10.1089/omi.2011.0118.
[36] T. Wu, E. Hu, S. Xu, M. Chen, P. Guo, Z. Dai, T. Feng, L. Zhou, W. Tang, L. Zhan, X. Fu, S. Liu, X. Bo, G. Yu, clusterProfiler 4.0: a universal enrichment tool for interpreting omics data, Innovation 2 (2021) 100141, https://doi.org/10.1016/j.xinn.2021.100141.
[37] K.A. Reynolds, E. Rosa-Molinar, R.E. Ward, H. Zhang, B.R. Urbanowicz, A. M. Settles, Accelerating biological insight for understudied genes, Integr. Comp. Biol. 61 (2021) 2233–2243, https://doi.org/10.1093/icb/icab029.
[38] The Gene Ontology Consortium, The Gene Ontology resource: enriching a GOld mine, Nucleic Acids Res. 49 (2021) D325–d334, https://doi.org/10.1093/nar/gkaa1113.
[39] E. Ulgen, O. Ozisik, O.U. Sezerman, pathfindR: an R package for comprehensive identification of enriched pathways in omics data through active subnetworks, Front. Genet. 10 (2019) 858, https://doi.org/10.3389/fgene.2019.00858.
[40] T.L. Pedersen, ggplot2, RDocumentation (2023). https://www.rdocumentation.org/packages/ggplot2/versions/3.4.2. (Accessed 18 July 2023).
[41] NC State University, Comparative Toxicogenomics database. https://ctdbase.org/, 2023. (Accessed 25 June 2024).
[42] O. Mancarcı, geneSynonym, GitHub (2023). https://github.com/oganm/geneSynonym. (Accessed 18 July 2023).
[43] G. Smyth limma, RDocumentation, version 3.28.14, 2016. https://www.rdocumentation.org/packages/limma/versions/3.28.14. (Accessed 18 July 2023).
[44] Swiss Institute of Bioinformatics, Gene expression data in animals. https://www.bgee.org/, 2023. (Accessed 20 July 2024).
[45] W. Luo, M.S. Friedman, K. Shedden, K.D. Hankenson, P.J. Woolf, GAGE: generally applicable gene set enrichment for pathway analysis, BMC Bioinf. 10 (2009) 161, https://doi.org/10.1186/1471-2105-10-161.
[46] W. Luo, Generally applicable gene-set/pathway analysis, Bioconductor (2024). (Accessed 20 July 2024).
[47] W. Luo, C. Brouwer, Pathview: an R/Bioconductor package for pathway-based data integration and visualization, Bioinformatics 29 (2013) 1830–1831, https://doi.org/10.1093/bioinformatics/btt285.
[48] M.A. Al Barashdi, A. Ali, M.F. McMullin, K. Mills, Protein tyrosine phosphatase receptor type C (PTPRC or CD45), J. Clin. Pathol. 74 (2021) 548–552, https://doi.org/10.1136/jclinpath-2020-206927.
[49] T. Yamashita, A. Sekiguchi, Y.K. Iwasaki, T. Date, K. Sagara, H. Tanabe, H. Suma, H. Sawada, T. Aizawa, Recruitment of immune cells across atrial endocardium in human atrial fibrillation, Circ. J. 74 (2010) 262–270, https://doi.org/10.1253/circj.cj-09-0644.
[50] M.S. Oh, J.Y. Hong, M.N. Kim, E.J. Kwak, S.Y. Kim, E.G. Kim, K.E. Lee, Y.S. Kim, H. M. Jee, S.H. Kim, I.S. Sol, C.O. Park, K.W. Kim, M.H. Sohn, Activated leukocyte cell adhesion molecule modulates Th2 immune response in atopic dermatitis, Allergy Asthma Immunol. Res. 11 (2019) 677–690.
[51] E. Dejana, F. Orsenigo, M.G. Lampugnani, The role of adherens junctions and VE-cadherin in the control of vascular permeability, J. Cell Sci. 121 (2008) 2115–2122, https://doi.org/10.1242/jcs.017897.
[52] M. Litviňuková, C. Talavera-López, H. Maatz, D. Reichart, C.L. Worth, E. L. Lindberg, M. Kanda, K. Polanski, M. Heinig, M. Lee, E.R. Nadelmann, K. Roberts, L. Tuck, E.S. Fasouli, D.M. DeLaughter, B. McDonough, H. Wakimoto, J. M. Gorham, S. Samari, K.T. Mahbubani, K. Saeb-Parsy, G. Patone, J.J. Boyle, H. Zhang, H. Zhang, A. Viveiros, G.Y. Oudit, O.A. Bayraktar, J.G. Seidman, C. E. Seidman, M. Noseda, N. Hubner, S.A. Teichmann, Cells of the adult human heart, Nature 588 (2020) 466–472, https://doi.org/10.1038/s41586-020-2797-4.
[53] Z. Hu, W. Liu, X. Hua, X. Chen, Y. Chang, Y. Hu, Z. Xu, J. Song, Single-cell transcriptomic atlas of different human cardiac arteries identifies cell types associated with vascular physiology, Arterioscler. Thromb. Vasc. Biol. 41 (2021) 1408–1427, https://doi.org/10.1161/ATVBAHA.120.315373.
[54] P.D. Price, D.H. Palmer Droguett, J.A. Taylor, D.W. Kim, E.S. Place, T.F. Rogers, J. E. Mank, C.R. Cooney, A.E. Wright, Detecting signatures of selection on gene expression, Nature Ecol. Evolu. 6 (2022) 1035–1045, https://doi.org/10.1038/s41559-022-01761-8.
[55] Y. Yura, S. Sano, K. Walsh, Clonal hematopoiesis: a new step linking inflammation to heart failure, JACC (J. Am. Coll. Cardiol.): Basic Transla. Sci. 5 (2020) 196–207, https://doi.org/10.1016/j.jacbts.2019.08.006.
[56] R. Engers, Tiam1, in: M. Schwab (Ed.), Encyclopedia of Cancer, Springer Berlin Heidelberg, Berlin, Heidelberg, 2011, pp. 3691–3694.
[57] N. Fujimura, B. Xu, J. Dalman, H. Deng, K. Aoyama, R.L. Dalman, CCR2 inhibition sequesters multiple subsets of leukocytes in the bone marrow, Sci. Rep. 5 (2015) 11664, https://doi.org/10.1038/srep11664.
[58] G. Gómez Hernández, M. Morell, M.E. Alarcón-Riquelme, The role of BANK1 in B cell signaling and disease, Cells (2021) 10, https://doi.org/10.3390/cells10051184.
[59] M. Wolfien, A.-M. Galow, P. Müller, M. Bartsch, R.M. Brunner, T. Goldammer, O. Wolkenhauer, A. Hoeflich, R. David, Single-nucleus sequencing of an entire mammalian heart: cell type composition and velocity, Cells 9 (2020) 318.
[60] X. Chen, Z. Zhang, G. Qiao, Z. Sun, W. Lu, Immune and inflammatory insights in atherosclerosis: development of a risk prediction model through single-cell and bulk transcriptomic analyses, Front. Immunol. 15 (2024), https://doi.org/10.3389/fimmu.2024.1448662.
[61] A.C. Bashore, H. Yan, C. Xue, L.Y. Zhu, E. Kim, T. Mawson, J. Coronel, A. Chung, N. Sachs, S. Ho, L.S. Ross, M. Kissner, E. Passegué, R.C. Bauer, L. Maegdefessel, M. Li, M.P. Reilly, High-dimensional single-cell multimodal landscape of human carotid atherosclerosis, Arterioscler. Thromb. Vasc. Biol. 44 (2024) 930–945, https://doi.org/10.1161/ATVBAHA.123.320524.
[62] M.A. Adelsman, Y. Shimizu, Adhesion molecules, in: P.J. Delves (Ed.), Encyclopedia of Immunology, second ed., Elsevier, Oxford, 1998, pp. 26–33.
[63] C. Binder, F. Cvetkovski, F. Sellberg, S. Berg, H. Paternina Visbal, D.H. Sachs, E. Berglund, D. Berglund, CD2 immunobiology, Front. Immunol. 11 (2020), https://doi.org/10.3389/fimmu.2020.01090.
[64] M.L. Hermiston, V. Gupta, A. Weiss, CD45, in: R.A. Bradshaw, E.A. Dennis (Eds.), Handbook of Cell Signaling, second ed., Academic Press, San Diego, 2010, pp. 743–748.
[65] N.Q. Tay, D.C.P. Lee, Y.L. Chua, N. Prabhu, N.R.J. Gascoigne, D.M. Kemeny, CD40L expression allows CD8+ T cells to promote their own expansion and differentiation through dendritic cells, Front. Immunol. 8 (2017), https://doi.org/10.3389/fimmu.2017.01484.
[66] Y.M. Hyun, C.T. Lefort, M. Kim, Leukocyte integrins and their ligand interactions, Immunol. Res. 45 (2009) 195–208, https://doi.org/10.1007/s12026-009-8101-1.
[67] A.C. Finney, K.Y. Stokes, C.B. Pattillo, A.W. Orr, Integrin signaling in atherosclerosis, Cell. Mol. Life Sci. 74 (2017) 2263–2282, https://doi.org/10.1007/s00018-017-2490-4.
[68] X. Pang, X. He, Z. Qiu, H. Zhang, R. Xie, Z. Liu, Y. Gu, N. Zhao, Q. Xiang, Y. Cui, Targeting integrin pathways: mechanisms and advances in therapy, Signal Transduct. Targeted Ther. 8 (2023) 1, https://doi.org/10.1038/s41392-022-01259-6.
[69] M. Schnoor, Endothelial actin-binding proteins and actin dynamics in leukocyte transendothelial migration, J. Immunol. 194 (2015) 3535–3541, https://doi.org/10.4049/jimmunol.1403250.
[70] B. Rowshanravan, N. Halliday, D.M. Sansom, CTLA-4: a moving target in immunotherapy, Blood 131 (2018) 58–67, https://doi.org/10.1182/blood-2017-06-741033.
[71] L.M. Schnapp, J.M. Breuss, D.M. Ramos, D. Sheppard, R. Pytela, Sequence and tissue distribution of the human integrin α8 subunit: a β1-associated α subunit expressed in smooth muscle cells, J. Cell Sci. 108 (1995) 537–544, https://doi.org/10.1242/jcs.108.2.537.
[72] C.M. Kitchen, S.L. Cowan, X. Long, J.M. Miano, Expression and promoter analysis of a highly restricted integrin alpha gene in vascular smooth muscle, Gene 513 (2013) 82–89, https://doi.org/10.1016/j.gene.2012.10.073.
[73] N.R. Tucker, M. Chaffin, S.J. Fleming, A.W. Hall, V.A. Parsons, K.C. Bedi, A.-D. Akkad, C.N. Herndon, A. Arduini, I. Papangeli, C. Roselli, F. Aguet, S.H. Choi, K. G. Ardlie, M. Babadi, K.B. Margulies, C.M. Stegmann, P.T. Ellinor, Transcriptional and cellular diversity of the human heart, Circulation 142 (2020) 466–482, https://doi.org/10.1161/CIRCULATIONAHA.119.045401.
[74] L. Osborn, C. Hession, R. Tizard, C. Vassallo, S. Luhowskyj, G. Chi-Rosso, R. Lobb, Direct expression cloning of vascular cell adhesion molecule 1, a cytokine-induced endothelial protein that binds to lymphocytes, Cell 59 (1989) 1203–1211, https://doi.org/10.1016/0092-8674(89)90775-7.
[75] L. Amalia, The role of platelet-selectin as a marker of thrombocyte aggregation on cerebral sinus venous thrombosis, J. Blood Med 13 (2022) 267–274, https://doi.org/10.2147/jbm.S356028.
[76] Z. Liu, Y. Huang, D. Wang, M. Li, Q. Zhang, C. Pan, Y. Lin, Y. Luo, Z. Shi, P. Zhang, Y. Zheng, Insights gained from single-cell RNA analysis of murine endothelial cells in aging hearts, Heliyon 9 (2023) e18324, https://doi.org/10.1016/j.heliyon.2023.e18324.
[77] C.F. Krieglstein, D.N. Granger, Adhesion molecules and their role in vascular disease, Am. J. Hypertens. 14 (2001) 44S–54S, https://doi.org/10.1016/s0895-7061(01)02069-6.
[78] J. Miao, K. Zhang, Y. Yang, S. Xu, J. Du, T. Wu, C. Tao, Y. Wang, S. Yang, Single-nucleus transcriptomics reveal cardiac cell type-specific diversification in metabolic disease transgenic pigs, iScience 27 (2024) 110015, https://doi.org/10.1016/j.isci.2024.110015.
[79] C.-P. Manta, T. Leibing, M. Friedrich, H. Nolte, M. Adrian, K. Schledzewski, J. Krzistetzko, C. Kirkamm, C. David Schmid, Y. Xi, A. Stojanovic, S. Tonack, C. de la Torre, S. Hammad, S. Offermanns, M. Krüger, A. Cerwenka, M. Platten, S. Goerdt, C. Géraud, Targeting of scavenger receptors stabilin-1 and stabilin-2 ameliorates atherosclerosis by a plasma proteome switch mediating monocyte/macrophage suppression, Circulation 146 (2022) 1783–1799, https://doi.org/10.1161/CIRCULATIONAHA.121.058615.
[80] S. Yanagi, R. Inatome, T. Takano, H. Yamamura, Syk expression and novel function in a wide variety of tissues, Biochem. Biophys. Res. Commun. 288 (2001) 495–498, https://doi.org/10.1006/bbrc.2001.5788.
[81] J.M. Bradshaw, The Src, Syk, and Tec family kinases: distinct types of molecular switches, Cell. Signal. 22 (2010) 1175–1184, https://doi.org/10.1016/j.cellsig.2010.03.001.
[82] R.P. Siraganian, R.O. de Castro, E.A. Barbu, J. Zhang, Mast cell signaling: the role of protein tyrosine kinase Syk, its activation and screening methods for new pathway participants, FEBS Lett. 584 (2010) 4933–4940, https://doi.org/10.1016/j.febslet.2010.08.006.
[83] J.E. Bradley, G. Ramirez, J.S. Hagood, Roles and regulation of Thy-1, a context-dependent modulator of cell phenotype, Biofactors 35 (2009) 258–265, https://doi.org/10.1002/biof.41.
[84] K.G. Oikonomou, K. Zachou, G.N. Dalekos, Alpha-actinin: a multidisciplinary protein with important role in B-cell driven autoimmunity, Autoimmun. Rev. 10 (2011) 389–396, https://doi.org/10.1016/j.autrev.2010.12.009.

[85] T.M. Bunnell, B.J. Burbach, Y. Shimizu, J.M. Ervasti, β-Actin specifically controls cell growth, migration, and the G-actin pool, Mol. Biol. Cell 22 (2011) 4047–4058, https://doi.org/10.1091/mbc.E11-06-0582.
[86] D.H. Broide, P. Sriramarao, Cellular adhesion in inflammation, in: N.F. Adkinson, B.S. Bochner, A.W. Burks, W.W. Busse, S.T. Holgate, R.F. Lemanske, R.E. O'Hehir (Eds.), Middleton's Allergy, eighth ed., W.B. Saunders, London, 2014, pp. 83–97.
[87] R.L. Silverstein, M. Febbraio, CD36, a scavenger receptor involved in immunity, metabolism, angiogenesis, and behavior, Sci. Signal. 2 (2009) re3, https://doi.org/10.1126/scisignal.272re3.
[88] J.D. Larson, S.A. Wadman, E. Chen, L. Kerley, K.J. Clark, M. Eide, S. Lippert, A. Nasevicius, S.C. Ekker, P.B. Hackett, J.J. Essner, Expression of VE-cadherin in zebrafish embryos: a new tool to evaluate vascular development, Dev. Dyn. 231 (2004) 204–213, https://doi.org/10.1002/dvdy.20102.
[89] J. Tang, H. Zhang, L. He, X. Huang, Y. Li, W. Pu, W. Yu, L. Zhang, D. Cai, K.O. Lui, B. Zhou, Genetic fate mapping defines the vascular potential of endocardial cells in the adult heart, Circ. Res. 122 (2018) 984–993, https://doi.org/10.1161/CIRCRESAHA.117.312354.
[90] H. Suryawanshi, R. Clancy, P. Morozov, M.K. Halushka, J.P. Buyon, T. Tuschl, Cell atlas of the foetal human heart and implications for autoimmune-mediated congenital heart block, Cardiovasc. Res. 116 (2019) 1446–1457, https://doi.org/10.1093/cvr/cvz257.
[91] H. Elmasri, C. Karaaslan, Y. Teper, E. Ghelfi, M. Weng, T.A. Ince, H. Kozakewich, J. Bischoff, S. Cataltepe, Fatty acid binding protein 4 is a target of VEGF and a regulator of cell proliferation in endothelial cells, FASEB J. 23 (2009) 3865–3873, https://doi.org/10.1096/fj.09-134882.
[92] N.G. Lambert, H. ElShelmani, M.K. Singh, F.C. Mansergh, M.A. Wride, M. Padilla, D. Keegan, R.E. Hogg, B.K. Ambati, Risk factors and biomarkers of age-related macular degeneration, Prog. Retin. Eye Res. 54 (2016) 64–102, https://doi.org/10.1016/j.preteyeres.2016.04.003.
[93] M.E. Pepin, R.M. Gupta, The role of endothelial cells in atherosclerosis: insights from genetic association studies, Am. J. Pathol. 194 (2024) 499–509, https://doi.org/10.1016/j.ajpath.2023.09.012.
[94] W.A. Muller, Transendothelial migration: unifying principles from the endothelial perspective, Immunol. Rev. 273 (2016) 61–75, https://doi.org/10.1111/imr.12443.
[95] H. Kang, X. Li, K. Xiong, Z. Song, J. Tian, Y. Wen, A. Sun, X. Deng, The entry and egress of monocytes in atherosclerosis: a biochemical and biomechanical driven process, Cardiovasc. Ther. 2021 (2021) 6642927, https://doi.org/10.1155/2021/6642927.
[96] O. Harki, S. Bouyon, M. Sallé, A. Arco-Hierves, E. Lemarié, A. Demory, C. Chirica, I. Vilgrain, J.-L. Pépin, G. Faury, A. Briançon-Marjollet, Inhibition of vascular endothelial cadherin cleavage prevents elastic fiber alterations and atherosclerosis induced by intermittent hypoxia in the mouse aorta, Int. J. Mol. Sci. 23 (2022) 7012.
[97] W.H. Wagner, R.M. Henderson, H.E. Hicks, A.J. Banes, G. Johnson Jr., Differences in morphology, growth rate, and protein synthesis between cultured arterial and venous endothelial cells, J. Vasc. Surg. 8 (1988) 509–519, https://doi.org/10.1016/0741-5214(88)90119-X.
[98] D. van Geemen, M.W.J. Smeets, A.-M.D. van Stalborch, L.A.E. Woerdeman, M.J.A. P. Daemen, P.L. Hordijk, S. Huveneers, F-Actin–Anchored focal adhesions distinguish endothelial phenotypes of human arteries and veins, Arterioscler. Thromb. Vasc. Biol. 34 (2014) 2059–2067, https://doi.org/10.1161/ATVBAHA.114.304180.
[99] D.K. Arnett, R.S. Blumenthal, M.A. Albert, A.B. Buroker, Z.D. Goldberger, E. J. Hahn, C.D. Himmelfarb, A. Khera, D. Lloyd-Jones, J.W. McEvoy, E.D. Michos, M. D. Miedema, D. Muñoz, S.C. Smith Jr., S.S. Virani, K.A. Williams Sr., J. Yeboah, B. Ziaeian, 2019 ACC/AHA guideline on the primary prevention of cardiovascular disease: executive summary: a report of the American College of Cardiology/American heart association task force on clinical practice guidelines, Circulation 140 (2019) e563–e595, https://doi.org/10.1161/cir.0000000000000677.